EFFECT OF HIGH-FREQUENCY PLASMA PYROLYSIS ON THE PHYSICOCHEMICAL PROPERTIES OF BIOCHAR

Lappeenranta–Lahti University of Technology LUT

Wroclaw University of Science and Technology in Poland (WUST)

University of Castilla-La Mancha in Spain (UCLM)

Master's Programme in Technology, Master's thesis

Master's programme Sustainable Biomass and Bioproducts Engineering

2024

Endashaw Workie Yihunu

Examiner(s): Professor Halina-Pawlak Kruczek

Ikenna Anugwom, D.Sc. (Tech.)

ABSTRACT

Lappeenranta–Lahti University of Technology LUT

LUT School of Engineering Sciences

Chemical and Process Engineering

In co-operation with partner university/universities: Wroclaw University of Science and Technology in Poland (WUST) and the University of Castilla-La Mancha in Spain (UCLM)

Endashaw Workie Yihunu

Effect of High-Frequency Plasma Pyrolysis on the Physicochemical Properties of Biochar

Master's thesis

2024

54 pages, 10 figures, 3 tables and appendix

Examiner(s): Professor Halina-Pawlak Kruczek and Ikenna Anugwom, D.Sc. (Tech.)

Keywords: Biochar, Biomass, Carbon, Characterization, Plasma, pyrolysis

Graphical Abstract

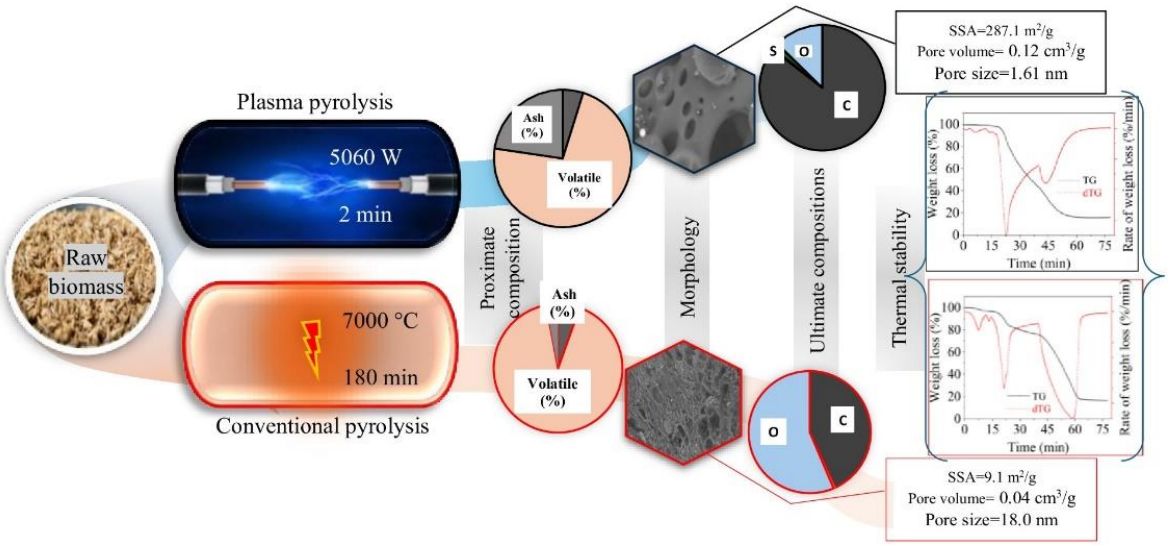

Biochar has distinct physicochemical properties, making it a subject of considerable significance in modern environmental research. The choice of production route is a key factor that affects the properties of biochar and its potential applications. This study explored the effect of plasma pyrolysis on the physicochemical properties of biochar. The resulting biochar product was then subjected to a comprehensive characterization. Briefly, proximate composition and thermal behavior were characterized using thermogravimetric analysis (TGA). Ultimate analyses were conducted via an elemental analyzer. The morphological changes were characterized by scanning electron microscopy (SEM), while specific surface area and pore size distribution were quantified using the Brunauer-Emmett-Teller (BET) model. Three different and representative biomasses, viz., Miscanthus, brewery spent grain (BSG), and smoke wood, were used as feedstock. As a reference, conventionally pyrolyzed biochar of each biomass type was utilized. The results show that plasma pyrolysis significantly reduces the volatile content of biochar across all biomass types by up to 68% while increasing ash content by as much as 9%, with smoke wood having the maximum volatile reduction and miscanthus having the highest change in ash content. TGA analysis revealed that plasma pyrolyzed biochar samples exhibited higher thermal stability, evidencing the late on-set temperature and high ash content, aligning with the proximate results. Interestingly, the specific surface area of plasma pyrolyzed biochar was found to be significantly lower, ranging from 7.07 to 9.06 m2/g, than the conventional counterpart, ranging from 287.15 to 488.39 m2/g. The total pore volume follows the same trend. However, a significantly broad pore size distribution was observed for plasma pyrolyzed biochar, attributed to the deformation of a network of microstructures that led to a low surface area and pore volume but enlarged pore size. The surface morphology further supports this notion since it reveals the lack of microporous structure and the predominance of meso- and macropores. A consistent increment of carbon content and aromaticity, with increases ranging from approximately 4% to 18% and a reduction of oxygen by up to 15% across all plasma pyrolyzed biochar, was observed. The findings of this study demonstrate that high-frequency plasma pyrolysis significantly affects the physicochemical properties of biochar, with slight differences across biomass types.

ACKNOWLEDGEMENTS

I wish to express my most sincere words of gratitude to all who gave me moral and technical support in the course of doing this MSc thesis. I want to start by thanking my supervisor, Professor Halina-Pawlak Kruczek, for giving me the opportunity to carry out this research and for her constant advice throughout the project. Secondly, I would like to express my sincere thanks to Dr. Krystian Krochmalny, who significantly contributed to the study described in this thesis. Without his experience, technical and substantive engagement, as well as enthusiasm, this thesis project would not have been completed as successfully. I am also thankful to Dr. Mateusz Kowal for his contributions and support. I thank my co-supervisor, Dr. Ikenna Anugwom, for his feedback. I would like to take this opportunity to thank the teaching and non-teaching staff of the faculty of mechanical and power engineering for setting up a highly motivating academic atmosphere and providing me with the utmost possible facilities to conduct my study. I am grateful to Erasmus Mundus for the financial assistance through which I completed this project. Lastly, I express my gratitude to my family and friends, whose continuous support and encouragement have always been with me over the years.

All credit goes to God‡ for His blessings in completing this research and on its path.

SYMBOLS AND ABBREVIATIONS

Superscripts

*	Calculated value
d	On a dry basis

Abbreviations

BCB	Conventionally pyrolyzed BSG biochar
BSG	Brewery Spent Grain
BPB	Plasma pyrolyzed BSG biochar
MCB	Conventionally pyrolyzed Miscanthus biochar
MPB	Plasma pyrolyzed Miscanthus biochar
WCB	Conventionally pyrolyzed Smoke wood biochar
WPB	Plasma pyrolyzed Smoke wood biochar
SEM	Scanning Electron Microscopy
TGA	Thermogravimetry Analysis
BET	Brunauer-Emmett-Teller
BJH	Barrett-Joyner-Halenda
DSC	Differential scanning calorimetry
dTG	Derivative of Thermogravimetry

Table of contents

Contents

Figures

Tables

1 Introduction

With increasing concern over climate change and resource depletion, biomaterials are now a focus of interest in various sectors. This is because biomaterials are derived from living things or biological processes, which potentially offer renewable and sustainable alternatives to fossil fuels and emission-intensive materials (Rosenboom, Langer and Traverso, 2022). Biochar is one of the promising biomaterials that has a long history of application, from soil amendment to tomb preservation (Chen et al., 2019). It is a pyrogenous, carbon-rich solid material obtained from the thermal conversion of various biomasses. In the modern day, biochar is mainly used for environmental remediation, including water treatment, soil amelioration and carbon sequestration (Wang and Wang, 2019). The quality and efficiency of biochar are largely determined by its physicochemical properties and the pyrolysis conditions. To date, several thermal-based processes such as pyrolysis, hydrothermal carbonization, torrefaction and gasification have been developed for biochar production (Gabhane et al., 2020). However, pyrolysis is the predominant technique for producing biochar because of its relative versatility and efficiency, yielding biochar with enhanced carbon content and stability. Pyrolysis can be performed in an oxygen-starved atmosphere at high temperatures (350-900 °C) in a specially designed reactor (Yaashikaa et al., 2020). However, contemporary pyrolysis techniques still present several drawbacks that can compromise the physicochemical properties of biochar required for various purposes.

Biochar obtained from the existing pyrolysis techniques usually has heterogeneous physicochemical properties, such as surface area, pore volume, functionality, and charge. Consequently, it becomes challenging to determine the precise characteristics of biochar for a particular application (Ippolito et al., 2020; Altıkat et al., 2024). This is due to the uneven distribution of heat throughout the biomass sample during conventional pyrolysis (Devi and Rawat, 2020; Nguyen and Khuong, 2022; Pahnila et al., 2023). Another reason associated with the existing pyrolysis technique is the limited control over the reaction conditions. For instance, achieving a specific pore structure can be difficult because of the uncontrolled nature of the process (Ippolito et al., 2020). Furthermore, conventional pyrolysis usually operates at very low reaction rates, which not only limit the amount of feed material that can be processed and prolong the processing time but also result in excessive thermal degradation of the biochar (Chen et al., 2016). This degradation might appear as changes in texture, morphology, and overall impact on its structural integrity and functional properties.

Given these limitations, there arises a pressing need to explore state-of-the-art methods for engineered biochar production.

Plasma pyrolysis is a cutting-edge technology primarily employed for plastic waste treatment (Bhatt et al., 2022). It is a thermal process that uses plasma to decompose materials at high temperatures and in a matter of seconds to minutes. Plasma is an ionized gas molecule and stream of electrons that is generated by applying a high-frequency electric field to the gas (Chen et al., 2022). The potential of this technology in biomass conversion, particularly for the purpose of producing biochar, has not been thoroughly studied and may be an innovative concept that merits more investigation.

In this study, it is hypothesized that, by subjecting biomass to a controlled plasma environment (hereafter plasma pyrolysis), it is possible to obtain biochar with enhanced physical and chemical properties and low environmental effects, which potentially results in superior efficacy for sequestering carbon and other applications.

2 Aim and Scope of the study

Aim

The aim of this study is to investigate the effect of high-frequency plasma pyrolysis on the physicochemical properties of biochar from different biomass residues.

Scope

The scope of this study encompasses reactor development, char production and characterizing the product. Briefly, a laboratory-scale prototype plasma pyrolysis reactor tailored for biochar production was designed, followed by the production of biochar using this reactor. The relevant physicochemical properties of the produced biochar considered for characterization are surface area and porosity analysis, morphology, thermal stability, proximate composition, ultimate composition and hygroscopicity. Concurrently, biochar obtained from the conventional pyrolysis reactor was used as a reference for the investigation of the physicochemical change brought about by the plasma pyrolysis reactor. Considering the cost and technical difficulties, optimization of operating conditions is limited to residence time only. Pertaining to the same factors, characterization of properties was limited to a biochar produced at a single time to be considered as optimal residence time. However, three deemed to be representative biomasses have been used as feedstocks to assess the effect of plasma pyrolysis across biomass verities.

3. State of the Art Review

3.1. Biochar: Overview

3.1.1. Definition

According to the European Biochar Certificate, “Biochar is a porous, carbonaceous material that is produced by pyrolyzing biomass and is applied in such a way that the contained carbon remains stored as a long-term C sink or replaces fossil carbon in industrial manufacturing” (EBC, 2012-2023). The name, biochar, itself emphasizes its origin from biomass, making it a renewable resource when produced sustainably. It is a charcoal-like substance with a high carbon content (50–90%), and the remaining is composed of ashes and minerals. Biochar is created in a thermo-chemical reactor in which temperatures between 200 °C and 1200 °C applied in oxygen-deprived environments, preventing the material from burning but converting it into a carbon-rich product (Penstate Extension, 2023).

3.1.2. History

Biochar is a solid biomaterial that comes through the carbonization of organic matter, and it has its roots in indigenous societies, mostly the pre-Columbian Amazonians. By then, it can be made through a slash-and-char process to gain terra preta, whose fertile soils enrich biochar and increase agriculture productivity while sequestering carbon (Nordic Biochar Network, n. d.). Although the usage of biochar dates to 2000 years ago, with its exact utilization possibly extending even further in time, the term "biochar" was coined in the late 20th century, and its application has grown worldwide (Chen et al., 2019). Thanks to several thermochemical processes involved, biochar is now made from any type of dry biomass these days, making it much more ecologically friendly compared to standard charcoal production. Since the year 2015, there has been a prominent increase in biochar being used in agriculture, with its use spreading to other sectors as well (Wu et al., 2023).

3.1.3. Application

Agricultural applications

Applying biochar for soil amendment has multifaceted benefits. Many studies have reported that it will enhance soil fertility, health and productivity by retaining essential nutrients and water, maintaining pH and cation exchange capacity (Alkharabsheh et al., 2021; Nepal et al., 2023). These enhanced physical conditions provide a more favorable habitat for microbial organisms, which are essential for nutrient recycling and plant growth.

Environmental application

One of the primary environmental applications of biochar is eliminating contaminants from aquatic systems. However, the chemical property of biochar highly influence its efficiency in removing organic contaminants. Hence, biochar that possesses a large surface area and micropores, a hydrophobic nature, and a low content of dissolved organic carbon will tend to have a high affinity for organic pollutants, thereby effectively removing them. Conversely, biochar with low surface area and micropores and low content of dissolved organic carbon will be effective in removing inorganic pollutants (Oliveira et al., 2017; Harrish and Pawar, 2022).

Biochar can also help to reduce the mobility of persistent organic pollutants (POPs) and other toxins that could potentially seep into groundwater. Thus, the presence of biochar in soil serves a dual purpose, maintaining the quality of both the soil and water (Qiu et al., 2022). Another important application of biochar is its potential for carbon sequestration. This function relates to the stable carbon content of biochar, which directly corresponds to the amount of CO_2 locked in its structure. Moreover, when applied to soil, it can capture a certain amount of CO_2 from the atmosphere and mitigate the release of non-CO_2 gases such as CH_4 and N_2O from soils (Li and Tasnady, 2023). Thus, biochar not only facilitates pollutant remediation but also serves as a potent approach for pollution reduction and augmenting carbon sequestration.

Industrial applications

Recently, biochar has also become an emerging input for various industries owing to its versatility and sustainability. For instance, it can be used as a reliable source of fuel in the renewable energy industry because of its high calorific value (Suman et al., 2018). Biochar can also be applied in bioelectrochemical systems to facilitate the promotion of electricity generation from organic wastes (You et al., 2021). Furthermore, it is used within building materials as a component, for example, in bricks and concrete, to improve their properties and sequester carbon within these materials (Osman et al., 2023). This has made biochar suitable for use in filtration and catalysis, making it an efficient medium in both processes.

3.2. Properties of biochar and characterization techniques

Following the definition, historical backdrop, and practical use of biochar, it is vital to explore its physicochemical properties, which make it a subject of considerable significance in modern environmental research. Biochar is often characterized by a multitude of physical

and chemical properties, including a high carbon content, an abundant surface area, a well-formed network of pores and good thermal resistance.

3.2.1. Chemical composition

Biochar boasts a superior carbon content, compared to the original feedstock, often exceeding 50% by weight (Tomczyk, Sokołowska and Boguta, 2020). This enrichment is achieved through the thermochemical conversion process, where volatile components are driven off, concentrating the stable carbon structures within the biochar matrix. The carbon content of raw biomass remains relatively constant within the range of 10-30% and does not change until it undergoes a certain degree of heat. Hence, the pyrolyzing temperature has a direct impact, where lower temperatures raise the fixed carbon content to 50-60% while higher temperatures increase the carbon content to 90% (Weber and Quicker, 2018). This is because high temperatures cause the thermal-induced conversion of biomass carbon molecules into stable and resistant carbon structures, resulting in aromatization and molecular ordering (Tomczyk, Sokołowska and Boguta, 2020). Crucially, since this carbon exists in a highly recalcitrant form, it resists degradation by microorganisms. This characteristic enables biochar to persist in the soil for decades or centuries, effectively sequestering and immobilizing carbon (Petersen et al., 2023).

Biochar is composed mainly of carbon, but it also contains other elements like nitrogen (N), oxygen (O), hydrogen (H), sulfur (S), and calcium (Ca). The percentage of these elements can be quantified using elemental analyzers. Accordingly, the sample is ignited at a temperature of 1000 °C using oxygen in its pure form. Subsequently, the elements C, N, H, and S are transformed into carbon dioxide, nitrogen oxide, water, and sulfur dioxide, respectively, followed by helium gas heating in a copper tube. The clean form of these converted compounds can then be measured via gas chromatography or by employing infrared and thermal conductivity cells (Świechowski et al., 2022).

3.2.2. Thermal stability and proximate composition

Understanding the thermal behavior and proximate composition of biochar is crucial to determining its specific intended application and behavior with a change in surrounding temperature. Biochar is proximately composed of moisture, volatiles, and ash. The moisture content is the amount of water retained in biochar which affects its weight, volume, reactivity and storage capacity. When the biochar is subjected to an intense temperature, some organic substances start to release in gaseous form, called volatile matter. When the biochar,

subsequently, undergoes a combustion stage, there will be a certain amount of inorganic substances remaining in the feedstock, called ash contents. Characterizing the volatile matters of biochar can provide insights into its thermal stability and reactivity of biochar while the ash and fixed carbon content of biochar may indicate its potential application, especially in the case of soil amendment, as they reveal the mineral content contained in the biochar (Maniraj et al., 2023).

The moisture content of biochar is directly correlates with its hygroscopicity and indirectly related to the pyrolysis temperature; a high pyrolysis temperature results in less moisture content, which indicates increased hygroscopicity of biochar, and the reverse is true (Jiang et al., 2021). Conversely, ash content tends to rise with increasing pyrolysis temperatures. Rafiq et al. (2016) observed that the ash content of corn-derived biochar increases exponentially when the pyrolysis temperature increases from 300 to 500 °C. This is caused by the progressive concentration of inorganics such as calcium, potassium, and other trace metals following the decomposition and volatilization of the cellulose and hemicellulose content of the feedstock at a faster rate (Tomczyk, Sokołowska and Boguta, 2020). It is widely stated that high ash content can negate the potential use of biochar, especially if intending to apply for carbon sequestration (Puri, Hu and Naterer, 2024).

Meanwhile, raising the temperature reduces the amount of volatile matter in biochar by breaking down volatile components into smaller liquid and gas molecules. This can also result in the desiccation of hydroxyl groups and the thermal decomposition of cellulose and lignin. Hence, lower volatiles mean a lower degree of thermal alteration undergone by biochar, which is favorably correlated with the stability of biochar (Tomczyk, Sokołowska and Boguta, 2020).

The thermal stability and proximate composition can be analyzed by using thermogravimetry (TGA) where the biochar sample is subjected to a programmed temperature range in an inert and/or oxidative atmosphere, and the equipment constantly measures the mass of the sample as the temperature rises. In this way, TGA provides a curve that shows the distinct stages at which the moisture loss, the volatile release, and the fixed carbon are combusted. The derivative of this result, also called derivative thermogravimetry (dTG), will be the rate of mass loss and particular thermal transitions.

3.2.3. Surface properties and porosity

The specific surface area and porosity of biochar are crucial factors that determine its quality and suitability for specific applications. Biochar with a surface area of below 250 m^2/g is

usually ideal for improving soil fertility, while biochar with a surface area over 500 m^2/g can be employed for purposes like adsorption, carbon sequestration, and energy production (Celignis, n. d.; Leng et al., 2021). The specific surface area and pore structure of biochar themselves are interdependent, with microspores being the most influential factor. The surface area of biochar usually falls within the range of 8 to 132 m^2/g, whereas its total pore volume is typically from 0.016 to 0.083 cm^3/g. The pore size distribution of biochar is commonly categorized into three groups: micropore (< 2 nm), mesopore (2-50 nm), and macropore (> 50 nm) (Leng et al., 2021).

These surface properties are significantly affected by the production systems, especially temperature, and the characteristics of raw feedstocks. For instance, increasing the pyrolysis temperature resulted in a more noticeable rise in microporosity and specific surface area, as well as a higher carbon and ash content (Batista et al., 2018; Tomczyk, Sokołowska and Boguta, 2020). This is primarily because the breakdown of cellulose and hemicellulose, generates more micropores and vascular bundles, or channeled structures, within biochar. The breakdown of lignin and the subsequent escape of volatile constituents further enhance the surface area and pore volume.

Surface area is usually quantified using Brunauer-Emmett-Teller (BET) model. This model involves calculating the quantity of gas physically adsorbed on the surface of the biochar at a fixed temperature and variable pressure. The determination of pore width and pore volume can be carried out by the Barrett-Joyner-Halenda (BJH) method and the t-plot method, respectively (Armah et al., 2022).

3.2.4. Morphology

The morphological structure of biochar is a complex interplay of its physical structure, particle size, shape, porosity, and chemical properties. Generally, the more pronounced networks of pores and higher specific surface area come with higher pyrolysis temperatures (Antonangelo et al., 2019). Feedstock composition also plays a key role in its inherent composition; for instance, lignocellulosic materials generally have fibrous biochar structures and high porosity, while those derived from agricultural residues may have more irregular and fragmented pore structures (Khawkomol et al., 2021). The scanning electron microscope (SEM) is an effective tool utilized to characterize the surface morphology of biochar at high resolution. This technique allows microstructural features to be visible, which are crucial for the properties and potentials of biochar in applications. During the process, the electrons are

released from the source, focused into a beam, and then interaction is made with a sample so as to generate signals. The signals provide information regarding surface topography, composition, or any other characteristic. Detectors, for example, secondary electron detectors, collect such signals and produce an image with high resolution of a sample to reveal its intricate morphology (Scimed, n. d.).

3.3. Production processes for biochar

The physicochemical properties of biochar discussed in Section 3.2 collectively determine its use in multiple sectors. Meanwhile, all these properties are intricately associated with two major factors: the biochar production route, mainly the temperature whereat pyrolysis occurs, and the kind of biomass utilized as feedstock. Both factors are responsible for obtaining a variant of biochar with its own unique characteristics and functionalities (Ippolito et al., 2020). The core of this study, however, delves into the effects of production methods. Figure 2 presents the operational parameters, such as residence time and pyrolyzing temperature of various methods, compiled from the literature (Yaashikaa et al., 2020; Elkhalifa et al., 2022; Y. Zhang et al., 2022; Rajput et al., 2024; Ravindiran et al., 2024).

3.3.1. Conventional production methods

Pyrolysis is the dominant and conventional technique employed to produce biochar (Yaashikaa et al., 2020). It is a thermo-chemical treatment process wherein biomass is subjected to a hot environment without or with very little oxygen. The typical range of pyrolysis temperatures is between 300 and 900 °C (Gabhane et al., 2020). The main biomass components, such as hemicellulose, decompose at 220 °C to 315 °C, cellulose at 315 °C to 400 °C, and lignin at 160 °C to 900 °C (Danesh et al., 2023). At the corresponding temperature level, these biomass components undergo reactions like cross-linking, depolymerization, and fragmentation and end up producing char, bio-oil, and a mixture of gases (syngas) (Cha et al., 2016).

Pyrolysis can be grouped into three categories: slow, fast, and flash. This categorization is determined by many operational parameters, such as temperature, heating rate, and reaction duration. Regarding yield, as shown in Figure 1, slow pyrolysis offers a higher solid (char) output than others, while fast pyrolysis offers a high liquid product (Al Arni, 2018). A lower heating rate (<10 °C/min) results in a stable char network due to slow devolatilization, while a higher heating rate leads to rapid evaporation and enhanced porosity. In terms of residence time, an increase in time results in a decrease in volatile matter and an increase in fixed

carbon (Gabhane et al., 2020). Pyrolysis can also be operated either in batch mode, the cheapest mode, which is widely practiced in rural areas, or in continuous mode which is favorable for commercial biochar production due to its high quality, energy efficiency, and maximum output (Panwar, Pawar and Salvi, 2019).

3.3.2. Emerging biochar production methods

Torrefaction

Pyrolysis is a well-researched and practically used technique for producing biochar, yet some emerging methods can potentially advance the production pathway. Torrefaction is one of these emerging techniques. In fact, torrefaction can be used as either a standalone production scheme or as a pretreatment for other techniques, depending on the intended purpose of the final product (Panwar, Pawar and Salvi, 2019). It is operated in the same process as conventional pyrolysis except being operated in a mild (200-300 °C) environment. In this process, the hemicellulose component of lignocellulosic biomass is primarily impacted owing to its amorphous structure and comparatively low level of polymerization (Patra *et al.*, 2021). Torrefaction is gaining significant interest due to its notable efficient use of energy and ability to produce biochar with enhanced hydrophobicity and energy density (Yadav and Singh, 2023).

Gasification

Although the primary aim of gasification is to produce syngas, it has also recently been used to produce biochar. The process requires a high temperature and anoxic environment to dry, pyrolyze, combust and reduce the feedstocks in sequence (Hussain et al., 2023). This means, in contrast to pyrolysis, gasification requires an extreme temperature (700–1100 °C) and favors the presence of oxygen which leads to a higher gaseous output than solids. Despite the gasification method being blamed for its low biochar yield, the produced char has a more stable (Hansen et al., 2015) and porous carbon content (Adeniyi, Ighalo and Onifade, 2021).

Microwave-assisted pyrolysis

Microwave pyrolysis is another potential technique for in-situ treatment of organic waste to obtain energy-based products like biochar, bio-oil, and syngas. Microwave heating is employed to attain elevated temperatures and rapid heat transfer for extensive decomposition. In microwave pyrolysis, unlike conventional pyrolysis, heat is produced inside the feedstock sample through controlled molecular motion caused by ionic vibration

and the rotation of dipolar molecules. This leads to rapid but uniform heating and high energy efficiency (Li et al., 2016; Azwar et al., 2022).

Xiang et al. (2022) reported that the microwave pyrolysis of biochar enhances both the specific surface area and pore volume. This enhancement was achieved by raising the microwave power and pyrolyzing temperature. However, the feed material may experience uneven absorption of microwave energy, resulting in the formation of hotspots and cold patches (Ke et al., 2024). In addition, microwave pyrolysis has lower energy for activation (E_A) than conventional production methods, making it a less sustainable alternative (Zhang et al., 2022).

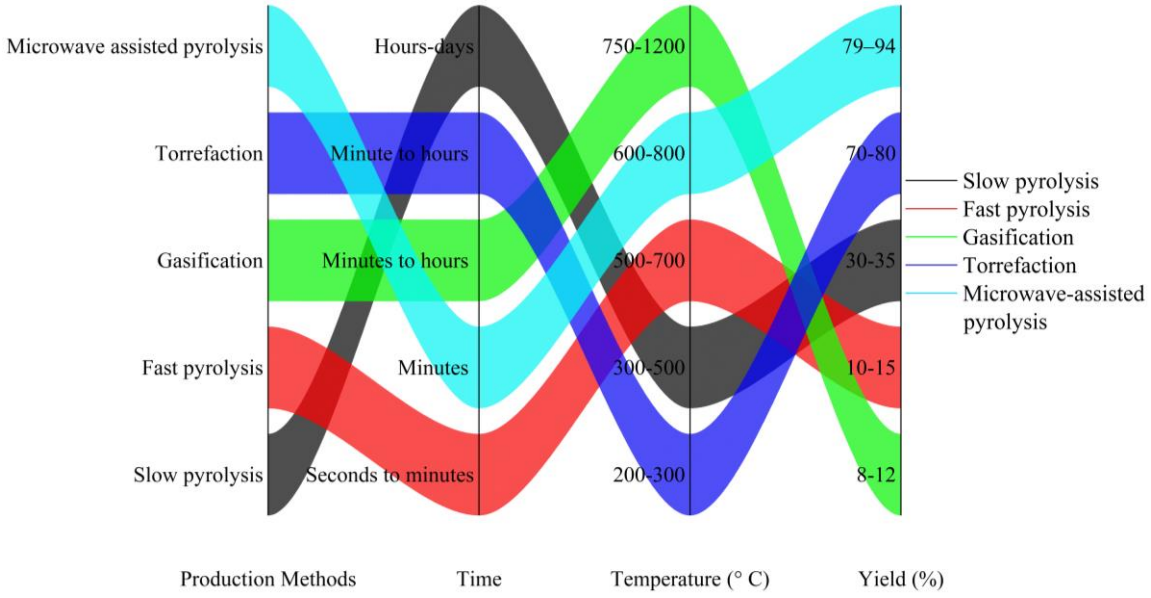

Figure 1. Operating time, temperature and yield of existing biochar production methods

3.4. Plasma Pyrolysis

3.4.1. Definition

Plasma pyrolysis is an advanced thermochemical conversion technology that can be used to disintegrate waste material into gases and char. It uses plasma to initiate the intense heat (>1500 K) required for decomposition and to catalyze the overall reactions in an inert atmosphere (Bhatt et al., 2022). Plasma, a fourth state of matter, is an electronically ionized gas composed of electrons, ions and neutral particles. Ions and electrons are produced by applying high power to the plasma carrier gas (Chen et al., 2022). Plasma can be produced naturally, such as by lightning and the northern lights or artificially, such as by lamps and plasma televisions (Agun et al., 2022). Plasma pyrolysis is a very fast process that can even be done within milliseconds. So far, it has been widely applied in plastic waste treatment owing to the efficient valorization of hazardous substances with low tar output and reduction

of waste volume (Bhatt et al., 2022). Hence, plasma pyrolysis is an eco-friendly technology that converts waste into energy and other valuable goods, promoting a circular economy.

3.4.2. Principles of Plasma Pyrolysis

Plasma pyrolysis works based on the principles of both plasma physics and chemistry. It follows the premise that extremely energetic plasma, which is the ionized state of gases, can effectively initiate and maintain chemical processes that involve the breakdown of feed material. Ionization of gas occurs when gas molecules are energized to the point that electrons are ripped away from atoms or molecules, resulting in a combination of ions, free electrons, and neutral particles, collectively known as plasma (Goebel and Katz, 2008). A substantial quantity of energy is emitted when the stripped electrons unite with the ionized species (Ganesh P., Nema and Jain, 2007). The charged particles then contain so much kinetic energy that they emit ultraviolet light as a form of energy (Bhatt *et al.*, 2022). To decompose complex molecules into simpler ones, this energy is transmitted directly to the substance, absorbed, and then used to break chemical bonds.

Plasma can be either thermal (hot) or non-thermal (cold). Thermal plasma pyrolysis utilizes intense temperatures to pyrolyze a feed material. Thermal plasma is defined by the fact that all its components have the same temperature, which is usually very high. What this means is that a thermal plasma can be described by a single temperature and its primary component consist of ions, electrons, and neutrals, all of which are in a state of thermodynamic equilibrium. Plasma torches operate at temperatures of a few thousand Kelvin, while fusion plasma devices and star interiors may reach temperatures of over a million Kelvin (SNEAD, 1999). Non-thermal plasma differs from thermal plasma in that it contains electrons with a much greater temperature compared to heavier ions and neutrals. This characteristic enables pyrolysis to occur at lower temperatures overall (Plasma-Universe, n. d.; Ganesh P., Nema and Jain, 2007; Bhatt et al., 2022). Evidencing its controllability, versatility and most importantly, conversion efficiency, thermal plasma pyrolysis would be a focus here (Palma *et al.*, 2020; Kwon and Im, 2022). As such, any mention of "plasma pyrolysis" throughout this text should be interpreted as referring only to thermal plasma, unless otherwise stated.

3.4.3. Mechanisms of plasma pyrolysis

In plasma pyrolysis, a series of complex reactions take place that alter the physicochemical characteristics of the feed material. The process begins with initiation in which a high-voltage power supply generates an arc between carbon or graphite electrodes. This arc is then stabilized by a gas stream and generates plasma (Daghagheleh *et al.*, 2023). Hence, the typical method used to produce thermal plasma is arc plasma. It is renowned for its high temperatures and thermal equilibrium (Ollegott *et al.*, 2020). Consequently, when ignited by a high-frequency electromagnetic wave, arc plasma could serve as an outstanding ignition source which allows the spark to be emitted from the torch tip without ever contacting sample material (Longevity, n. d.).

The high frequency here is a type of start-up ignition mechanism for plasma pyrolysis. The pioneering advantage of introducing this mechanism is that it rapidly and uniformly produces a thermal field, thereby providing good ionization or excitement efficiency (Li *et al.*, 2017; Agun *et al.*, 2022). The ionizing gases allow them to flow in the reactor to serve as a medium for the electric field and create an inert atmosphere. Following the excitement phenomenon, reactive species such as radicals, ions, excited atoms, and molecules are formed that can proactively interact with the sample material to facilitate the decomposition process (Aminu, Nahil and Williams, 2022). Hence, the sample material introduced into the plasma reactor breaks down into non-leachable solid residues and gaseous components. The most significant influencing factors on products and/or byproducts are the pyrolyzing temperature and time, the characteristics of feedstocks, the power supply, and the loading rate of feed. Typically, the pyrolysis of material, for example, solid waste, in a plasma process adheres to the reaction mechanism (Bhatt *et al.*, 2022) shown below in Figure 2.

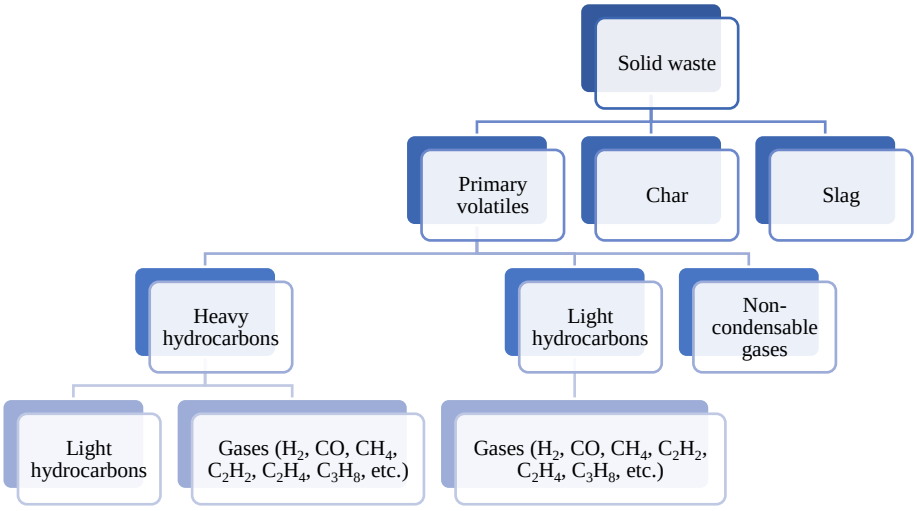

Figure 2. The typical mechanisms in the plasma pyrolysis of biomass

All these reaction mechanisms occur in the plasma zone and are very fast, complex and mostly simultaneous. It is noteworthy to mention that in the case of wet feedstock or the presence of steam, the char will be converted to H_2, CO and slag (Bhatt *et al.*, 2022).

3.4.4. Design of a Plasma Reactor

From a chemical engineering point of view, the intended reaction kinetics are affected by the suitability of the reactor design. Being a state-of-the-art technology, plasma pyrolysis has no one-size-fits-all design configuration yet. However, it is commonly designed with the integration of several components, each contributing to the efficiency of the overall conversion process. The high-power supply unit is the major component that should be robust enough to provide consistent electrical power to sustain the ionization process so that the plasma will also be sustained (Daghagheleh *et al.*, 2023). Central to the reactor, plasma arc/torch generating electrodes are introduced in proper arrangement, commonly as a counter electrode and front electrode that constitute an electric field and ionizing gases such as argon or nitrogen to produce high-energy plasma (Agun *et al.*, 2022). Argon is used to provide a stable plasma environment and prevent unfavorable chemical reactions (SCIPlasma, 2023). Nitrogen is abundant and can create a non-oxidizing environment, which is essential for preventing the combustion of feed materials (Chen et al., 2021). Whichever ionizing gas is used, the flow path must be regulated using a series of mass flow controllers. This is due to the necessity of creating a stable plasma and its behavior, consequently achieving the desired chemical environment of the pyrolysis process (Wheeler *et al.*, 2012).

Another core component is the reaction chamber where biomass interacts with plasma and is designed to withstand the very high temperatures produced by the plasma (Cheng *et al.*, 2015). The chamber is also accompanied by the flow path of the gases to be ionized, so they are well distributed and utilized in the pyrolysis process (Wheeler *et al.*, 2012). The real-time pyrolyzing temperature at the reaction chamber can be monitored by inbuilt thermocouples or through an external device such as optical emission spectroscopy (OES) and infrared (IR) thermography (Wnukowski, 2023). This is essential to ensure consistent heat transfer and avoid overheating the reactor. To further safeguard the reactor and maintain an elevated temperature, it is necessary to implement cooling systems and/or insulators properly. The cooling system might consist of a heat exchanger or air cooling to effectively disperse excessive heat from the chamber and the generated gases (Zhai *et al.*, 2023). Insulators minimize heat loss from the system and shield exterior components from very high temperatures within the chamber. In large-scale pyrolysis reactors, feed mechanisms and product removal may be built for the constant feeding of feedstock to the reaction chamber and effectively collecting the output.

4. Methodology

4.1. Materials and apparatus

Biomass feedstocks

- Commercially purchased smoke wood chips
- Locally collected Miscanthus grass
- Wroclaw University of Science and Technology, Faculty of Chemistry donated Brewer's Spent Grain (BSG)

Plasma reactor (prototype) components

- Custom-made AC power supply (Operating frequency: 75kHz AC, Voltage: 800 V, Current 10A)
- Graphite electrode
- Chamber: stainless steel cylinder (outer), clay pot (middle) and parabolic base graphite pot (inner)
- Thermocouple (50-250 range, Termo Precyzja, Poland)
- DC motor (Groschopp & Co. KG, Mot KM 87-60 P23, Germany)
- Driveshaft

Conventional pyrolysis

- Rectangular tube furnace (Germany)

Chemicals

- Analytical grade N_2 (99.99%)

4.2. Designing Plasma reactor

Plasma pyrolysis is a state-of-the-art technology that has been used merely in non-organic material treatment. Hence, this work brought a prototype plasma pyrolysis reactor that was specifically designed to process biomass samples. A multi-layered chamber is designed to provide optimal thermal insulation and, hence, very good performance. The upper layer is made of cylinder-shaped, high-quality stainless steel with a port on the side to introduce an inert gas. Beneath this steel shell, there is a padded layer of thick cotton that prevents heat from dissipating out of the reactor, thus maintaining the temperature inside the reactor. Following the insulation material, there is a middle chamber made of clay with a fitted lid

that encases the innermost layer of the chamber. The inner chamber is made of carbon which can be considered a central component of the system as the biomass sample to be pyrolyzed will be placed in it. The choice of carbon-made chamber installation is attributed to its high-temperature resistance and electrical conductivity. Furthermore, carbon has relevant chemical compatibility, particularly its inertness which make it unlikely to react with the feedstock. A rotation mechanism was also introduced here, which enables the inner-chamber to be rotatable aiming to promote adequate and uniform exposure of the samples to the plasma arc. For this purpose, an external DC motor has been installed that drives a shaft through a chain drive (Figure 3). Furthermore, an adjustable stand was built to tilt up the reactor at some angle to facilitate heat distribution and provide easier access for maintenance and monitoring.

The plasma arc that converts the biomass to biochar is produced via a high frequency power supply. This power supply sends high-frequency alternating current (AC) to the electrode. Briefly, the power source is connected from two directions, with one connection at the front side of the electrode and the other extending from the rear side to the tip of the shaft. In other words, the front electrode, where the arc originates, functions as an active electrode while the deriving shaft that is bound to the inner chamber serves as the counter electrode or the ground point. Thus, the drive shaft has a dual role: as a counter electrode to complete the circuit by maintaining continuous current flow and to rotate the inner chamber that carries the feed material. Basically, this setup enables the flow of a high electric field along the active electrode ionizing the surrounding gases (N_2) and forming plasma from the active electrode to the counter electrode, which sandwiches the feed material in an intense and inert environment. Then, the current flows back through the shaft to the power supply, completing the circuit. To control the temperature in real-time, a thermocouple probe was equipped that extends to the inner chamber. The reactor is built with a dual-inlet gas port and a separate exhaust gas port. The former allows the supply of inert gas to ensure an oxygen-free environment while the latter will facilitate the expulsion of syngas and sample gas testing.

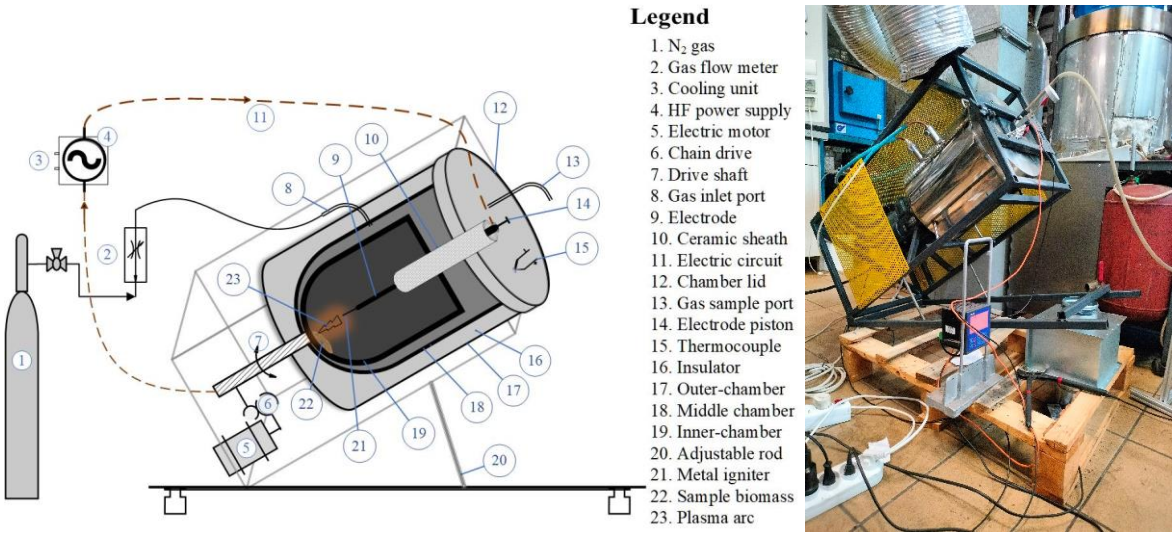

Figure 3. Layout (left) and actual image of a prototype plasma reactor for biochar production

4.3. Biochar production

Plasma pyrolyzed biochar is produced through the designed pyrolysis reactor. The reaction times varied from 1 min to 3 min, with 1 min intervals to observe the effect on the biochar properties. Three different biomass samples were selected to evaluate the plasma effect across various biomass types. All samples were received on a dry basis. The biomass samples were crushed to small particle sizes to obtain a uniform size. The crushed sample was subjected to an oven-dry for 1 hour and 100 °C prior to feeding to the reactor.

For the pyrolysis, 30 g of each of these raw samples was fed into the designated chamber of the plasma reactor. The N_2 flow rate was maintained as per conventional pyrolysis standards found in the literature. The plasma was then initiated at a high-frequency voltage of 550 V and a power of 9.2 ± 0.2 A. The electrode was positioned close to the sample to initiate plasma formation. Following the end of the desired residence time, the plasma generation was terminated, and the reactor cooled down under N_2 flow. Once cooled, biochar was taken out and kept in a plastic bag for subsequent characterization. The physical dynamics of the system, like the small particle size and the intense plasma sparks, led to dispersion and adhesion to the chamber wall rendering the collection and quantification of the biochar impractical. As a result, the mass balance study was ignored in this instance, acknowledging the limitations it presents in the precision of the pyrolysis yield data.

As a reference, conventionally pyrolyzed biochar was also produced under an inert atmosphere in a rectangular muffle furnace at 700 °C for 3 hours. This provided a benchmark to compare the changes in characteristics of biochar produced via plasma pyrolysis.

4.4. Product characterization

Prior to the production of biochar, the basic properties of raw biomass were characterized and presented in Table 1. Then, biochar obtained from plasma pyrolysis and conventional pyrolysis was characterized to investigate the physical (surface area, porosity, morphology and hygroscopicity), chemical (proximate and ultimate composition), and thermal (stability) changes in response to each production method. Briefly, an initial proximate analysis was performed on all samples, and one biochar sample was selected for further characterization from each biomass type and production route with the most favorable proximate composition. The proximate analysis included the ash content, volatile matter, moisture content and fixed carbon of biochar. The fixed carbon content represents the solid carbon residue following the removal of moisture, volatiles, and ashes and is indirectly calculated from these components using Eq. 1.

$$Fixed\ carbon^{d}(\%) = 100 - [Volatile\ content^{d}(\%) - Ash\ content^{d}(\%)] \quad (1)$$

Micromeritics® Accelerated Surface Area and Porosimetry (ASAP) 2020 (Micromeritics Instrument Corporation, USA) were employed to analyze the textural change of biochar. For this purpose, the impurities absorbed by the biochar were first removed through degassing the char in a vacuum at high temperatures. Then, the Brunauer-Emmett-Teller (BET) and Barrett-Joyner-Halenda (BJH) theories were applied to quantify the specific surface area and pore size distribution of biochar, respectively. The average pore size was estimated using a simplified cylindrical pore model that does not include interconnected pore networks (Li *et al.*, 2017; Ambroz *et al.*, 2018). The total pore volume of biochar was derived from the N_2 adsorption-desorption isotherms at liquid nitrogen (77K) and specific relative pressure ($P/P_0 = 0.99$). The t-plot approach was employed to compute the micropore volume and mesopore surface area. The mesopore volume was calculated by taking the difference between the micropore volume and the total pore volume. The morphological characterization was performed using a scanning electron microscope (SEM) (Hitachi TM-3000, Japan) at an accelerated voltage of 1.15 kV and various magnifications.

The ultimate composition of biochar was characterized using a CHNS/O analyzer (PerkinElmer®, USA). The sample was ignited at a temperature of 900 °C before analysis. Subsequently, the elements C, N, H, and S are transformed into carbon dioxide, nitrogen oxide, water, and sulfur dioxide, respectively. The helium gas is heated through a copper tube while unwanted gases are removed. Clean gases are quantified via a thermal conductivity detector (Świechowski *et al.*, 2022). Oxygen content was determined by Eq. 2.

$$Oxygen\ (\%) = 100 - [C\ (\%) + H\ (\%) + N\ (\%) + S\ (\%)] \quad (2)$$

The thermal stability and graphical decomposition pattern of samples were analyzed using a thermogravimetric analyzer (Setaram Setsys Evolution®, DTA/DSC SETARAM). The analysis was conducted from an ambient temperature to 700°C under inert gas (N_2), with a heating rate of 50 °C/min. Following a 15-minute exposure at 700 °C, the atmosphere was switched to O_2 to induce combustion thereby completing the thermal decomposition profile of the biochar samples. Simultaneously, derivative thermogravimetry (dTG) and differential scanning calorimetry (DSC) were applied to measure the rate of mass reduction detect distinctive thermal degradation occurrences, and assess the heat flow characteristics, respectively.

Table 1. Comprehensive analysis of the raw feedstocks

Characteristics	Parameters	Miscanthus	Smoke wood	BSG
Proximate composition (%)	Moisture	3.94	7.51	5.56
	Volatiles[d]	77.24	78.43	75.41
	Ash[d]	4.09	0.31	2.45
	Fixed carbon*	18.67	21.26	22.14
Ultimate composition (%)	C	49.00	44.88	48.09
	H	4.81	3.59	5.33
	N	0.65	0.53	4.14
	S	0.15	0.26	0.12
	O*	45.39	50.74	42.32
Higher calorific value (MJ/Kg)		18.12	17.93	18.45
Bulk density (Kg/m^3)		294.30	226.00	352.10

*Calculated value

[d]On a dry basis

4.5. Data analysis

The ultimate and proximate characterizations were carried out in double and average results were considered for further analysis. The data analyses were done in such a way that emphasized the changes in the biochar physicochemical properties brought by plasma pyrolysis over conventional pyrolysis. Hence, no direct comparison was made between plasma pyrolyzed biochar and conventionally pyrolyzed biochar. For brevity, each biochar product is strategically named as the first letter of the biomass name with the corresponding production method: MPB, BPB, and WPB for plasma pyrolyzed miscanthus biochar, plasma pyrolyzed brewery spent grain biochar and plasma pyrolyzed smoke wood biochar, respectively. Likewise, MCB, BCB, and WCB for conventionally pyrolyzed miscanthus biochar, conventionally pyrolyzed brewery spent grain biochar, and conventionally pyrolyzed smoke wood biochar, respectively.

5. Results and Discussions

5.1. Proximate analysis and thermal behavior

5.1.1. Proximate analysis

Proximate analysis refers to the process of determining the basic composition of a substance or material. As can be seen in Table 2, notable differences are shown in the moisture content, volatile matter, ash residue, and fixed carbon content between plasma pyrolyzed biochar and conventionally pyrolyzed biochar.

Table 2. Proximate composition of biochar samples

Biomass	Method of pyrolysis	Moisture (%)	Volatile[d] (%)	Ash[d] (%)	Fixed carbon[d] (%)
Miscanthus	Conventional	4.74	75.46	3.74	20.8
	Plasma	3.56	68.31	7.26	24.43
Smoke wood	Conventional	7.52	81.53	0.21	18.26
	Plasma	0.49	13.24	5.94	80.82
BSG	Conventional	4.54	75.72	2.45	21.83
	Plasma	2.43	36.53	11.42	52.05

The moisture content of biochar is an essential factor that affects its stability and storage. The findings demonstrate a decrease in moisture content when using plasma pyrolysis in contrast to conventional techniques. The moisture content of smoke wood and BSG significantly decreases from 7.52% and 4.54% with conventional pyrolysis to 0.49% and 2.43% using plasma pyrolysis, respectively. This is due to the intense temperature and energy input of plasma pyrolysis which can drive off the moisture thoroughly (Uroić Štefanko and Leszczynska, 2020). The significant reduction in moisture content suggests that plasma pyrolysis yields biochar with fewer hydrophilic sites and a more hydrophobic surface. This phenomenon may be explained by the alterations in surface functional groups, viz., the reduction in the concentration of oxygen-containing functional groups and the development of a more stable carbon matrix. These changes make the material less susceptible to moisture absorption (Bao *et al.*, 2021; Costa *et al.*, 2024). Subsequently, the energy density of biochar is enhanced due to its shrinkage, making it more efficient for specific applications such as fuel and energy production (John *et al.*, 2023). However, no significant difference was found for MPB, indicating that it was independent of the type of production method. This might be attributed to the unique chemical makeup or intrinsic physical structure of the raw material (Tomczyk, Sokołowska and Boguta, 2020).

Another important proximate composition of biochar indicating its thermal stability and reactivity is the volatile matter content. In comparison to conventional pyrolysis, plasma pyrolysis yields far fewer volatile compounds across all biomass types (Table 2). It is plausible that the high temperature and rapid quenching in plasma pyrolysis allowed for the complete devolatilization of volatile components and prevented secondary reactions, viz., cracking of primary pyrolysis products which is often caused by a prolonged reaction time, respectively. Saeed et al. (2016) stated that the increasing/decreasing trend of volatile matters can be associated with the heating rate applied up to a critical point. Thus, plasma pyrolysis is a preferred approach for producing biochar with low volatile matter, as it significantly reduces the volatile content.

Ash content corresponds to the solid mineral residue left after oxidative pyrolysis and correlates with the nutritional value of biochar. Plasma pyrolysis consistently and significantly enhanced the ash content of all biochar samples. With plasma pyrolysis, the ash content of miscanthus, BSG and smoke wood increases from 3.74% to 7.26%, 2.45% to 11.42%, 0.21% to 5.94%, respectively. This enhancement suggests the effective decomposition of complex organic compounds by plasma pyrolysis, resulting in high concentrations of inorganic constituents in the remaining char matrix (Ippolito *et al.*, 2020; Li *et al.*, 2023).

Fixed carbon content is a crucial parameter to assess the stability of biochar. It is calculated from the remaining proximate parameters and therefore it only accounts for the carbon content in the solid residue. According to the results (Table 2), plasma pyrolysis significantly increases the amount of fixed carbon in all types of feedstocks. The observed increase in fixed carbon content can be traced to a more complete carbonization process, yielding biochar with improved calorific value and enhanced ability for long-term carbon storage. This is supported by studies reporting that as the breakdown of organic compounds accelerates at an elevated temperature, a higher quantity of fixed carbon content can be achieved (Murtaza *et al.*, 2024). Briefly, this phenomenon is attributed to: first, the formation of char structures with a higher fixed carbon content due to increased devolatilization (Zhang *et al.*, 2019), second, the increase in biochar carbon-to-oxygen ratio due to the start of deoxygenation and dehydrogenation reactions (Yang *et al.*, 2024), and third, the development of condensed aromatic structures (Wu *et al.*, 2017). Soil amendment, carbon storage, and sustainable energy generation are some of the specific applications that benefit from these characteristics (Vilas-Boas *et al.*, 2024).

5.1.2. Thermal stability

The proximate analysis discussed in Section 5.1.1 was further examined by incorporating TGA results. The TGA results for biochar produced via plasma and conventional pyrolysis reveal notable differences in their thermal decomposition patterns over time and temperature.

The weight loss over the temperature curve in Figure 4 (a, c, e) shows the notable loss pattern started at 100 °C likely due to moisture release or low-molecular-weight volatile compounds and all plasma pyrolyzed biochar samples exhibit lower initial mass loss. This corresponds to the lower moisture content of plasma pyrolyzed biochar previously identified in the proximate analysis. By contrast, the mass loss of BPB started very steeply, a reflection of its higher moisture content. This trend carried on consistently until around 400 °C, at which point the weight loss was significantly different across both production methods and biomass types. This distinct trend corresponds to a devolatilization stage where plasma pyrolyzed biochar of all biomass types showed less weight loss because of its low volatile content, compared to conventionally pyrolyzed biochar. However, the magnitude of the change in weight loss was different across the biomass types where BPB exhibits a low deviation from its conventional counterpart while MPB possesses a high difference compared to MCB.

During the combustion stage, all samples showed a shock weight loss until the final ash content was obtained, regardless of production method and biomass types, owing to the vigorous breakdown of organic constituents. In this stage, the volatile matter and the majority of lignin components undergo rapid oxidation which contributes to huge weight loss. Following the burning of organic components, BSG and Miscanthus biochar from both methods ended up with nearly the same content of ash. This is not the case for WPB where it had a higher ash content, which aligns with its proximate composition. This might be attributed to their slower rate of devolatilization and more continuous mass loss with increasing pyrolysis temperatures (Tomczyk, Sokołowska and Boguta, 2020). Furthermore, the comparable high residual mass percentage of this biochar generally underscores the significant inherent mineral presence in the raw biomass (Xu *et al.*, 2023), irrespective of the production method. The ash content differences can be clearly seen in the weight loss over time curve provided in the Appendix.

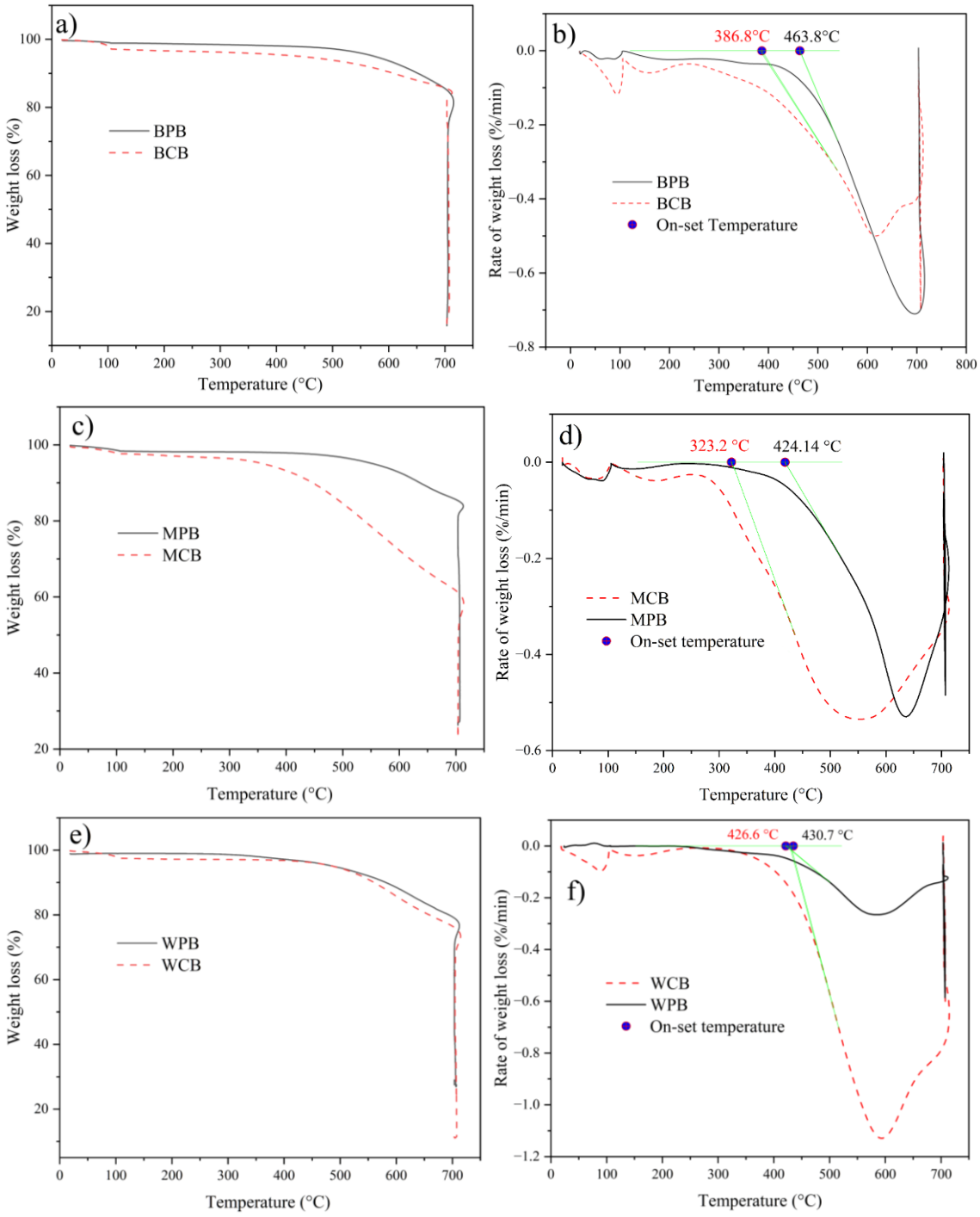

Figure 4. The TG (a, c, e) and dTG (b, d, f) profiles of plasma pyrolyzed biochar and conventionally pyrolyzed biochar from different biomass

The dTG curves in Figure 4 (b, d, f) provided further insights into the decomposition kinetics. Until the on-set temperature, the dTG mirrors the TG curve for all samples except for BPB and MPB which show a minor upward peak at the dehydration stage. In addition, for all plasma pyrolyzed biochar, the on-set temperature was late by about 100 °C, compared to the

conventionally pyrolyzed samples. A notable difference in the rate of weight loss between plasma pyrolyzed and conventionally pyrolyzed biochar was observed after 400 °C. BPB and MBP displayed a similar pattern with a lower and narrower peak in this region, suggesting a slower decomposition rate and potentially a more thermally stable organic matrix [40]. For WPB, while the on-set temperature was a bit later than even BPB and MPB, the dTG curve showed a broader and shallower peak at approximately 600 °C, indicating a more rapid and extensive decomposition of volatile matter in this sample. This major degradation phase is characterized by the decomposition of the main polymeric structure, or more recalcitrant lignin structures (Tomczyk, Sokołowska and Boguta, 2020). These findings agree with the TGA curve analysis.

Overall, evidencing the TG and dTG profiles, plasma pyrolysis consistently produces biochar with reduced moisture and volatiles, and increased fixed carbon, leading to greater thermal stability. The underlying mechanisms responsible for the better thermal performance of plasma-pyrolyzed biochar are anticipated to be the driving force. Briefly, during plasma treatment, the biochar constituents undergo cross-linking and polymerization, which results in increased rigidity of the biochar structure and consequently enhances its thermal resistance (Devi and Rawat, 2020). One possible mechanism attributed to this effect could also be the formation of char layers promoted by the high-energy environment of plasma, which would prevent further degradation.

5.1.3. Heat flow analysis

The DSC analysis further reveals the heat flow behavior of all biochar samples across a range of temperatures. Evidencing the thermogram presented in Figure 5, both plasma pyrolyzed and conventionally pyrolyzed biochar show consistent heat flow dynamics at the initial heating phase, specifically until 260 °C. Hence, all biochar samples heated up or cooled down in the same trend until this temperature range. Within this temperature range, three significant peaks are shown in order across all biomass types regardless of the pyrolysis method. The first endothermic peak was around 100 °C which corresponds to a dehydration stage where the moisture retained in the pores of biochar gets evaporated (Zoghlami and Paës, 2019). A second exothermic peak at about 140 °C indicates the decomposition of some low molecular weight organic components and the evaporation of bound water from the biomass structure. Following this exothermic peak, an endothermic peak at about 240 °C appears, caused by the decomposition of more labile components of the biomass, such as hemicellulose. These peaks may also reflect the formation of intermediate compounds owing

to the formation of more complex chemical structures through plasma pyrolysis. The slightly less or highly pronounced peaks across the pyrolysis methods and the biomass types suggest the amount of these components present in the samples (Vanisree, Chandran and Aparna, 2024).

In all cases, at higher temperatures, plasma biochar appears to have different mechanisms involved in heat transfer. Besides, the thermal signatures of the DSC plots for each type of biomass are unique because of the different chemical compositions of the respective biomasses. All these unique signatures point out that the effects of plasma pyrolysis on different types of biomasses imply that this method could be further optimized to obtain specific tailor-made characteristics. For BPB, plasma biochar exhibits a sharper exothermic peak around its on-set temperature (i.e., 460 °C). Prior to this thermal event, however, it exhibited a prominent exothermic peak at approximately 335 °C, indicating a more stable structure with fewer volatiles, likely due to the rapid and intense conditions of plasma pyrolysis. This exothermic transition reflects the decomposition of more thermally stable components or the release of energy from crystallization processes (Michigan State University, n.d.). In other words, plasma pyrolysis may alter the chemical composition such as the condensation of aromatic hydrocarbons or the structural properties of the biochar such as graphitization of the biochar. Briefly, during plasma pyrolysis, high temperatures can cause extensive cracking of biomass components, resulting in the production of aromatic hydrocarbons. As these hot aromatic molecules cool within the biochar matrix, they condense and release heat (exothermic) (Wnukowski, 2023). The high temperatures of plasma pyrolysis can also promote the rearrangement of the amorphous carbon structure in the biochar towards a more ordered, graphite-like structure (Devi and Rawat, 2020; Maniraj *et al.*, 2023). However, for both MPB and WPB, no significant exothermic peak was observed; instead, a wide endothermic peak was introduced for WBP. The broadness and highness of such a peak reflect that it is probably from the oxidative thermal degradation of residual organic components, leading to a release of huge energy. In WPB, the initiation of this thermal event is much later than in MPB, which is due to its high lignin content (Chakraborty *et al.*, 2021). Interestingly, MPB behaves with smooth heat flow at high temperatures, suggesting a steady state and predictable heat flow behavior (Nair *et al.*, 2023). Some spikes or anomalies in the heat flow curve could be associated with biochar purity, compositional differences, or structural irregularities.

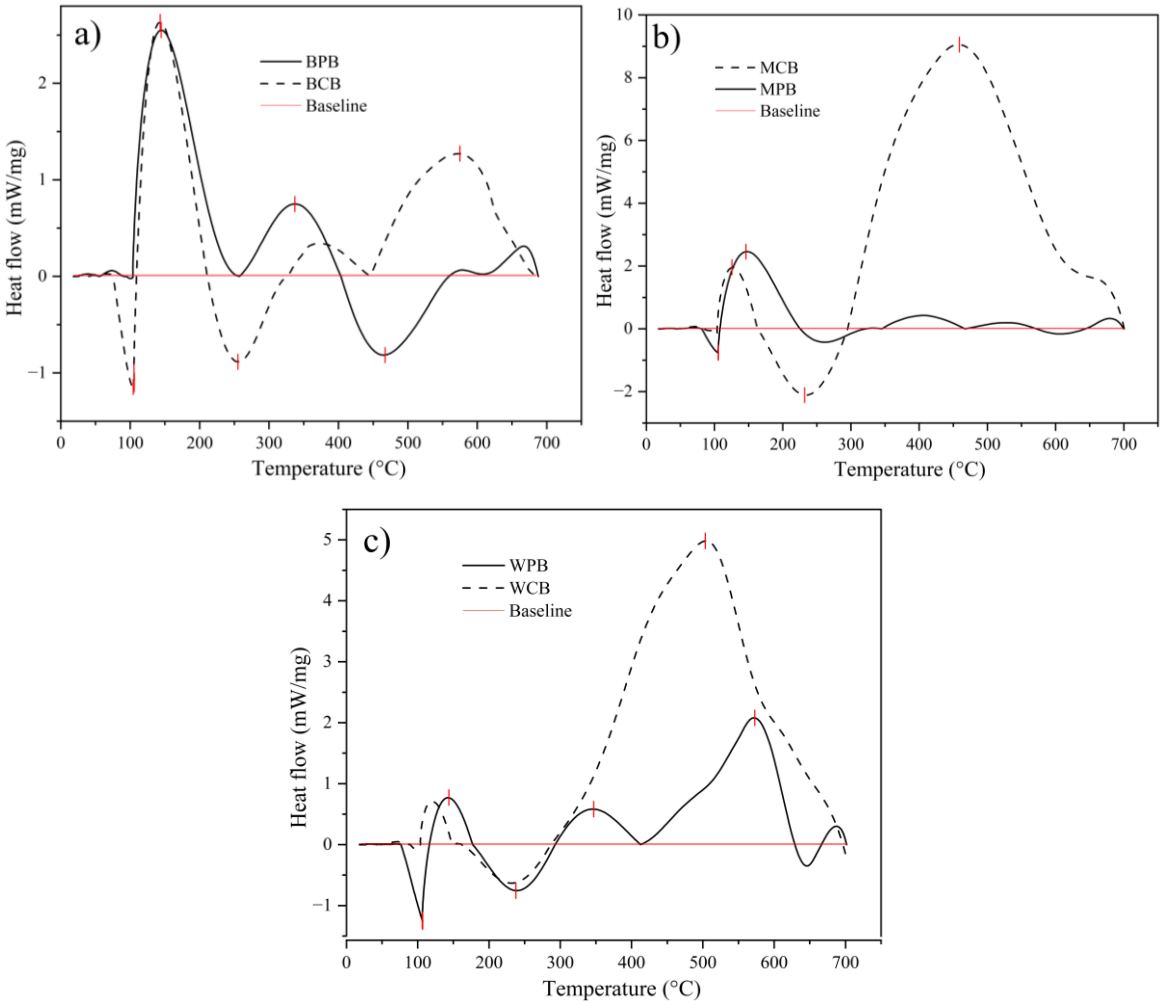

Figure 5. The DSC curve for a) BSG, b) Miscanthus and c) Smoke wood derived biochar

It is also noteworthy that extending the temperature range of the DSC measurement could reveal more endothermic or exothermic peaks associated with biochar component decomposition. Nevertheless, the DSC analysis shows a significant influence of plasma pyrolysis on the dynamics of heat transfer, which thermally changes the decomposition profile of biochar with conventional pyrolysis. Therefore, plasma pyrolysis enhances the thermal stability of biochar, while also causing decomposition to be more complex and resulting in the formation of unique carbonaceous structures.

5.2. Surface property analysis

5.2.1. Surface area and porosity

Adsorption of N_2 was carried out to identify the specific textural characteristics, and the BET method was used to estimate the surface area and pore volume. N_2 adsorption is a commonly practiced standard approach for surface area and porosity analysis since it provides isotherm

data that enables quantitatively determining the specific surface area and pore size distribution of a given sample material such as biochar. Figure 6 portrays the N_2 adsorption -desorption isotherms of the biochar samples studied.

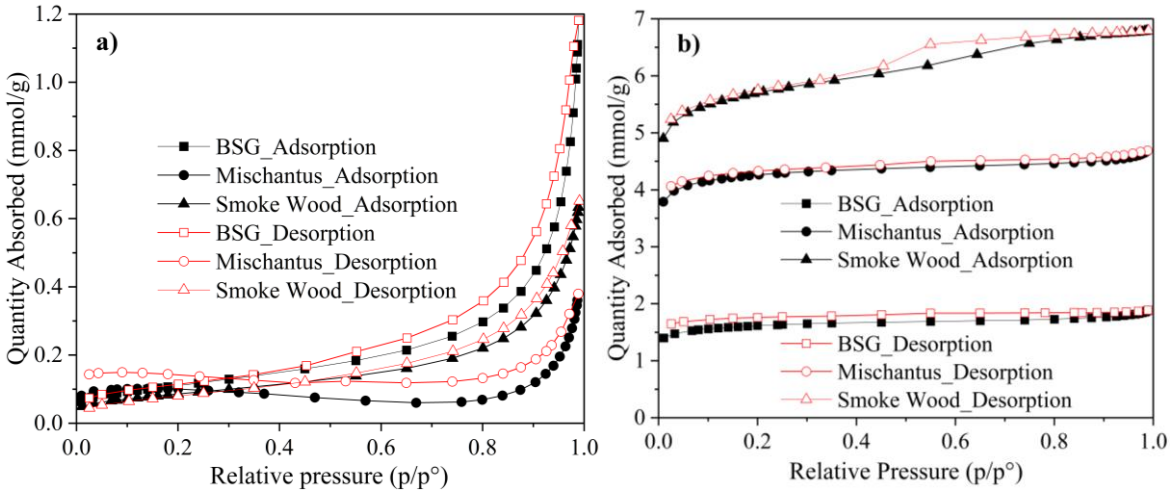

Figure 6. The nitrogen adsorption-desorption isotherms of (a) plasma pyrolyzed biochar and (b) conventionally pyrolyzed biochar

The adsorption rate of material (biochar, in this study case) is well recognized to be significantly impacted by its surface area and porosity. The higher the specific surface area, the higher the rate of adsorption (Zakaria *et al.*, 2017). From Figure 6, the adsorption rate at low P/P^0 values for the plasma pyrolyzed biochar is less observable than those for the conventionally pyrolyzed biochar of all types of biomasses. In addition, for plasma pyrolyzed biochar, the behavior of adsorption-desorption isotherms changed. According to the IUPAC classification, the N_2 isotherm for plasma pyrolyzed biochar adheres to type III, where sharp adsorption capacity implies that a relatively broad distribution of pore sizes has occurred, including narrower micropores and wider mesopores. It further suggests capillary condensation because of the small hysteresis loop in the adsorption-desorption isotherm, which in turn supports the mesoporous nature of plasma pyrolyzed biochar (Galarneau *et al.*, 2003). On the other hand, the isotherm of conventionally pyrolyzed biochar falls into a mixed type, namely isotherms I and IV (Rahman *et al.*, 2019). The type I isotherm corresponds to a micropore structure, whereas a type IV isotherm implies a combination of micropore and mesopore structures. The initial phase of the isotherms has a type I pattern, characterized by a substantial rise in adsorption at low relative pressures. This indicates that adsorption is occurring within micropores. At moderate to high levels of pressure, the isotherms exhibit a type IV isotherm pattern with a hysteresis loop classified as H4. This phenomenon is a result

of subsequent monolayer-multilayer adsorption, along with the presence of capillary condensation in small, narrow openings (Rahman et al., 2019).

Table 3 presents the specific surface area, total pore volume, and pore size distribution of all biochar samples. The result suggests that the BET-specific surface area for plasma pyrolyzed biochar of all biomass types is significantly lower than that of conventionally pyrolyzed chars. The result is consistent among all biomasses.

Table 3. Quantitative textural properties of different biochar samples

Parameters	BPB	BCB	MPB	MCB	WPB	WCB
SSA(m^2/g)	9.06	287.15	8.80	376.18	7.07	488.39
Total pore volume (cm^3/g)	0.04	0.12	0.01	0.16	0.02	0.24
Pore diameter (nm)	18.09	1.61	5.98	1.73	12.80	1.93

A t-plot analysis was carried out to characterize the microporous structure of the biochar further. This is a graphical method used to quantify the volume of micropores and the external surface of materials (Scherdel, Reichenauer and Wiener, 2010). In addition, the total pore volume from BET theory was estimated from the t-plot shown in Figure 7 and presented numerically in Table 3. The findings confirm that the total BET pore volumes for plasma pyrolyzed biochar were significantly lower than those for conventionally pyrolyzed biochar, regardless of biomass type.

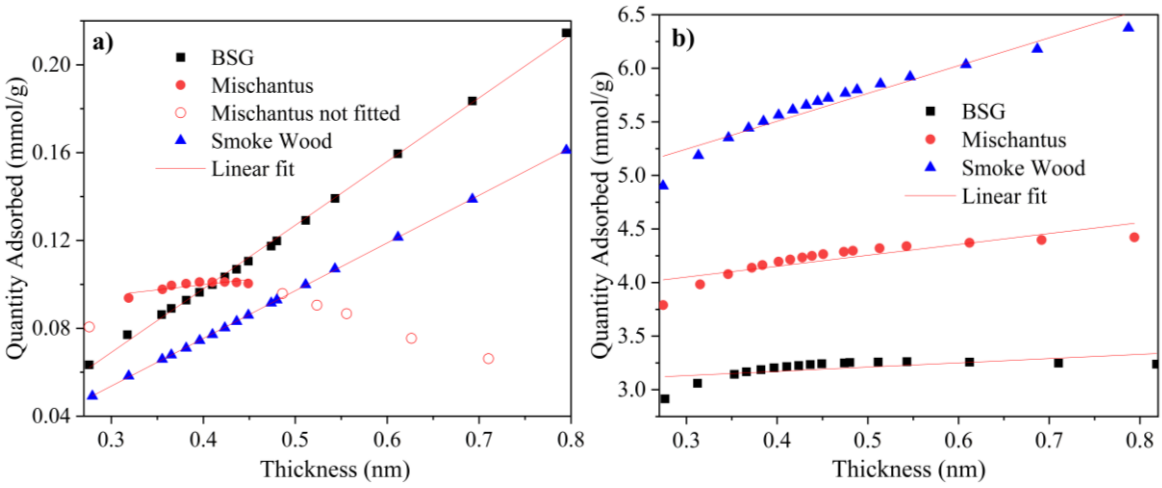

Figure 7. t-plots of (a) plasma pyrolyzed biochar and (b) conventionally pyrolyzed biochar

It is evident that the Y-intercept values in t-plot diagrams (proportional to the micropore volume parameter) for conventionally pyrolyzed biochar samples are positive, indicating the presence of micropores in these samples, as was conculcated from the N_2 adsorption-desorption isotherms. However, for the plasma pyrolyzed biochar (except the Miscanthus),

the Y-intercept values from the origin are negative, suggesting the absence of micropores. In t-plot diagrams, the slope of the line represents the external surface area of the analyzed samples (Scherdel, Reichenauer and Wiener, 2010). Accordingly, the external surface areas for the BPB, MPB, and WPB were 10.045, 1.650, and 7.527 mmol/g, respectively. Whereas the external surface areas for the BCB, MCB, and WCB were 13.758, 35.223, and 90.044 mmol/g, respectively. The result indicates that plasma pyrolyzed biochar demonstrated a significantly lower external surface area. From the t-plots, the micropore volume of, for example, MPB was 0.003 cm^3/g while the MCB was 0.130 cm^3/g. The mesopore volume was taken as the difference between the total BET pore volume and the micropore volume, assuming negligible macropores were available. Accordingly, the mesopore volumes for MBP and MCB were 0.019 and 0.032 cm^3/g, respectively. Therefore, the t-plot shows that plasma pyrolyzed biochar possesses the lowest micropore volume, consistent with the lower SSA and the total pore volume observed.

Pore size was defined based on the IUPAC standard as follows: micropore (< 2 nm wide), mesopores (2-50 nm wide), and macropore (> 50 nm wide). Micropores can be further subcategorized into ultramicropores, having a width of < 0.5 nm, and super-micropores, having a width of 1-2 nm (Rahman et al., 2019).

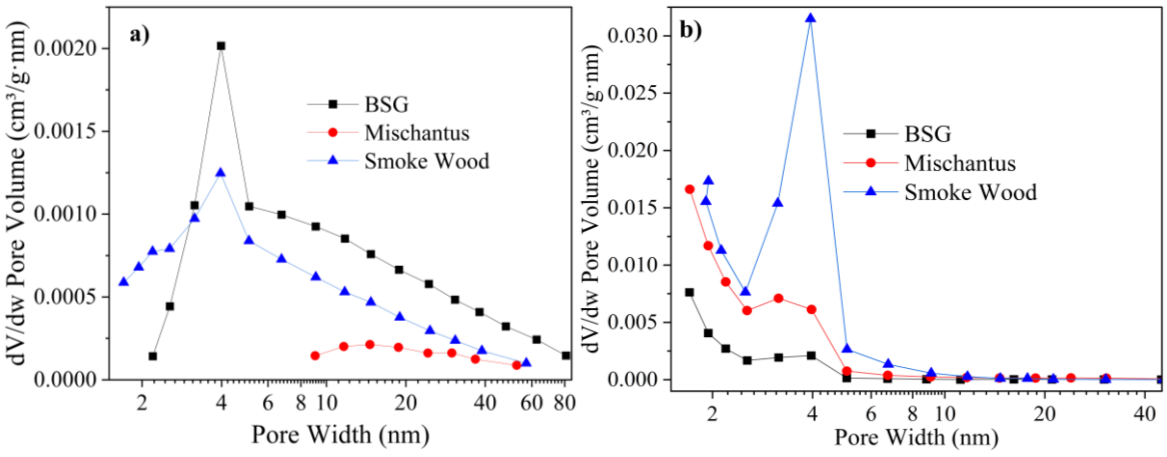

Figure 8. BJH plots of (a) plasma pyrolyzed biochar and (b) conventionally pyrolyzed biochar

Interestingly, the plasma pyrolyzed biochar consistently results in a wider pore width distribution across all biomasses, as illustrated in Figure 8. Table 3 also shows the higher average pore diameter of plasma pyrolyzed biochar. This result is further confirmed by the BET theory, demonstrating the enlargement of pore size and lack of micropores in the plasma pyrolyzed biochar. According to the BJH theory, for the BPB, MPB, and WPB, the

cumulative BJH desorption surface area of pores from 1.7 nm to 300 nm width were found to be 11.26, 1.37, and 8.73 cm^2/g, respectively, and their corresponding cumulative BJH desorption pore volume was 0.004, 0.008 and 0.021 cm^3/g. These values for the BCB, MCB and WCB were found to be 13.14, 22.815, and 90.12 cm^2/g, and 0.009, 0.021, and 0.074 cm^3/g, respectively. Hence, the smallest pores belong to the plasma pyrolyzed biochar. Essentially, plasma pyrolysis yields biochar with a significantly low surface area and low pore volume with larger pores than conventional pyrolysis. This textural change by plasma pyrolysis can be attributed to one or more of the following phenomena:

i) *Rapid heating and structural collapse:* Plasma pyrolysis is a super-fast process where the heating rates can reach above 1000°C in a matter of seconds. This results in an immediate thermal shock and volatile organic compounds released from the structural building blocks of biomass, including cellulose, hemicellulose, and lignin (Lu and Zong, 2018; Tomczyk, Sokołowska and Boguta, 2020; Regina et al., 2024). The cellular structure further collapses due to this rapid devolatilization before a stable network of micropores can be formed. In other words, the high pressure of gas together with the severe degree of thermal shock enlarges micropores to merge, and thus only a few pores are left, but larger. Consequently, plasma pyrolysis produced biochar with low microporosity, leading to a significantly reduced specific surface area and total pore volume.

ii) *Gas phase reactions:* In contrast to conventional pyrolysis, plasma pyrolysis drives intense gas-phase chemical reactions. This reaction would again cause the release of different volatile compounds (Rajput et al., 2024). Eroding the biochar matrix in this way can leads to the formation of new, bigger pores, and the collapse of smaller structures. Subsequently, the biochar matrix gradually wore away, resulting in the deformation of smaller structures while simultaneously expanding the pre-existing pores and creating new, larger ones.

iii) *Surface chemistry alterations:* Since plasma contains several reactive chemical species, it might introduce huge amounts of or other different functional groups, for example, oxygen-containing groups to the surface of biochar. These species then agglomerate and weaken the wall of pores, thereby contributing to the deformation of micropores and the formation of large pores (Peng et al., 2021; Ren et al., 2023). The reactive species may also induce cross-linking reactions, leading to a more rigid carbon matrix.

The findings also confirm that the change in texture characteristics among biomass types was consistent. However, it is noteworthy to mention that the magnitude of the change

differed. For example, Miscanthus had the minimum variations in SSA, pore volume and pore size between plasma pyrolyzed biochar and conventionally pyrolyzed biochar, while smoke wood showed the smallest. In addition, it can also be ascertained that WPB and BPB exhibited a unimodal pore size distribution, which is characteristic of the dominance of mesopores. Conversely, MPB contained a broader distribution, hence being characteristic of the heterogeneity of pore structure. This may be explained by the inherent differences in the chemical makeup, and cellular structure of these types of biomasses and their consecutive responses during the pyrolysis process.

5.2.2. Surface morphology

The effect of plasma pyrolysis on the morphology of biochar from different biomass feedstocks was further characterized by an SEM and shown in Figure 9. The SEM images reveal distinct morphological differences between plasma pyrolyzed biochar and conventionally pyrolyzed biochar. For example, MPB is characterized by a predominantly smooth surface interspersed with grooved fissures and some longitudinal fibrous structures appearing as undulating patterns. The MCB, on the contrary, reveals a very porous structure with a diverse range of pore sizes and channels. The surface features elongated, coalesced channels alongside irregularly shaped, jagged pieces. These channel-like cracks displayed in MCB are associated with its organized crystalline cellulose microfibrils (Sahoo et al., 2021). The morphological structure of BSG and smoke wood had relatively similar features, corresponding to both plasma pyrolysis and conventional pyrolysis. BPB and WPB are characterized by visibly opened but sparse pores with smoother overall texture and fewer irregularities. The meso- and macropores are evident as some visible and spherical round-edge-shaped pores distributed randomly. The smooth regions between the pores suggest a less complex surface morphology (Fang et al., 2020). BPB and WPB develop several cater-like cavities and pits without discernible pore formation. The lack of micropores and roughness, and dominance of microporosity in plasma biochar is consistent with its low SSA and pore volume as determined by BET measurements. Nonetheless, plasma biochar can potentially be used for applications that require bulk characteristics and flow-through capabilities, for example, filtration systems that require large pore channels. In contrast, both BCB and WCB biochar exhibit a high density of micropores and interconnected voids, further confirming its high surface area and pore volume, along with complex pore structures. This characterizes the fractured and heterogeneous texture of the biochar surface.

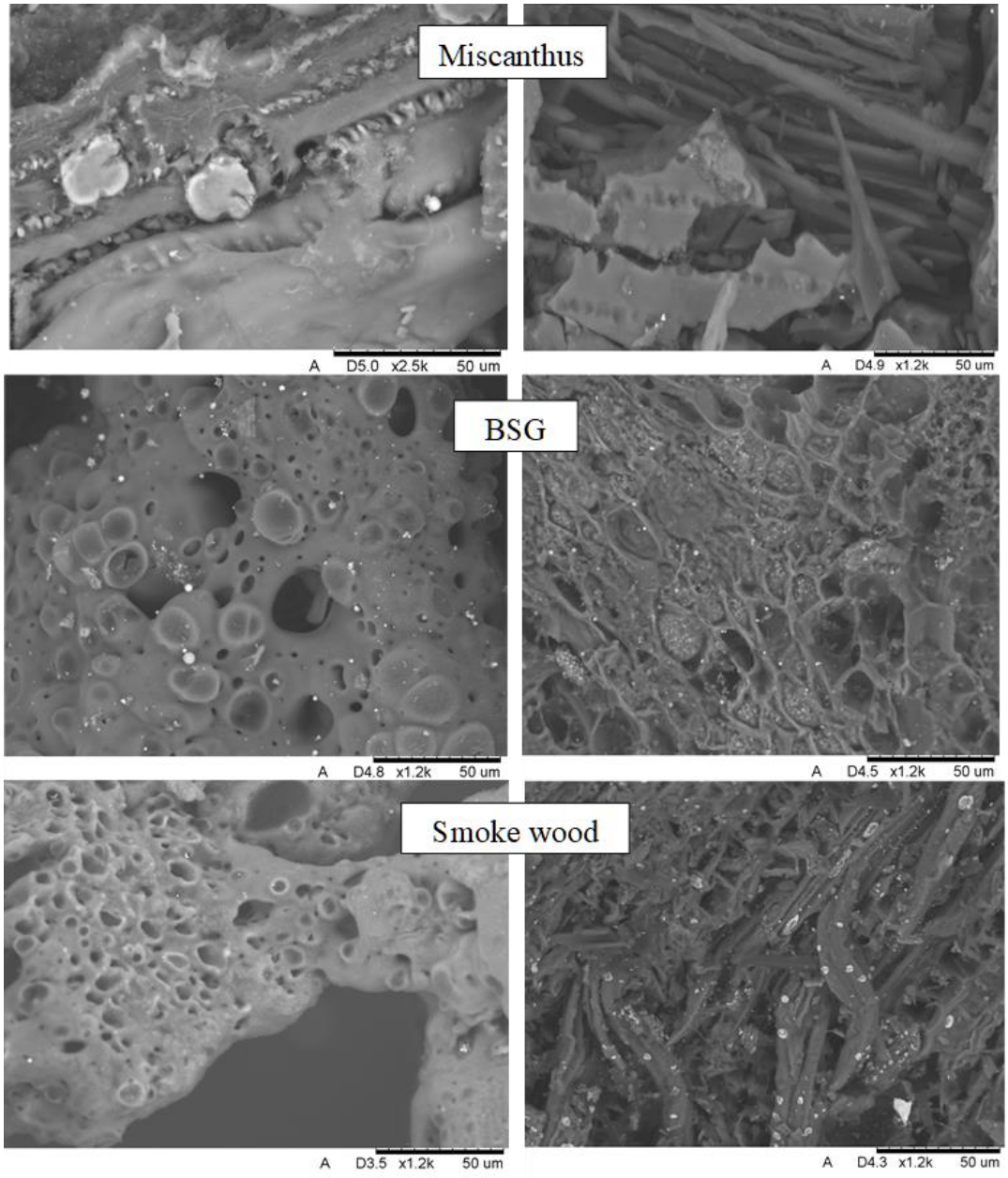

Figure 9. SEM visualization of morphology of plasma pyrolyzed (left) and conventionally pyrolyzed (right) biochar

5.3. The ultimate analysis of biochar

The analysis of the ultimate composition of plasma pyrolysis exhibits significant transformations across all biomass types, enhancing carbon retention and distinctively altering other elemental concentrations. According to Figure 9, MPB resulted in a 3.6% carbon content increase over the conventional counterpart, underscoring its efficacy in boosting carbon yield. On the other hand, for hydrogen, a slight difference was shown for hydrogen, nitrogen and sulfur content whereas the latter two were increased on plasma pyrolyzed biochar. Besides the carbon content, another significant difference was spotted

for the oxygen content at which MPB resulted in a 4.2% reduction in the oxygen content of miscanthus-derived biochar.

Smoke wood undergoes a significant change when subjected to plasma pyrolysis since it exhibits the most dramatic transformation in its chemical composition. The carbon content had a significant increase, rising from 77.1% to 88.3%, demonstrating a remarkable enhancement. There was a reduction in the hydrogen content, from 0.57% to 0.33%, and a notable rise in the nitrogen content, from 0.29% to 0.66%. The sulfur content experienced a significant increase, rising from 0.07% to 0.12%, whereas the oxygen level underwent a drastic decrease, dropping from 21.9% to 9.9%.

Plasma pyrolysis also significantly improved carbon retention for BSG, increasing its carbon content from 63.8% to 81.5%. The hydrogen and nitrogen content dropped from 0.95% to 0.36% and 3.9% to 1.6%, respectively. However, the sulfur content rose from 0.04% to 0.13%, whereas the oxygen content declined from 31.1% to 16.4%. Accordingly, plasma pyrolysis significantly enhances carbon content across all biomass types, with the most pronounced effect observed in wood and BSG. Such a dramatic elevation indicates a more efficient breakdown of organic matter into carbon-rich residues during plasma pyrolysis. Indeed, any thermal conversion process operated under elevated temperatures could result in the complete decomposition and volatilization of complex organic molecules, leaving behind highly carbonized biochar (X. Zhang et al., 2022; Ferraro et al., 2024). However, some underlying mechanisms of plasma pyrolysis might be responsible for the observed ultimate compositional changes. This includes decreased hydrogen content in all types of biomasses, which can be related to extreme temperatures that could drive off volatile chemicals, most probably in the form of hydrocarbons and water vapor. This was supported by a significant reduction in oxygen content for all biomass types (Siddiqui et al., 2022).

The modest increase in nitrogen content indicates that nitrogenous compounds show less volatility under plasma pyrolysis, particularly in Wood and Miscanthus (Alvarado-Flores et al., 2024). In addition, the high-energy plasma environment enables the inclusion of nitrogen into stable char structures, potentially through the formation of nitrides or other nitrogenous molecules that are stable in the carbon matrix. There is a slight rise in sulfur content across all forms of biomass. This may be ascribed to the creation of enduring sulfur compounds

that persist in the solid state even under elevated temperatures instead of undergoing vaporization (Miškovičová et al., 2024). The increased sulfur content found in all plasma pyrolyzed char samples provides evidence to support this notion.

The most significant justification was a substantial reduction in oxygen content across all biomass types. The elevated temperature, along with the reactive plasma environment of plasma pyrolysis facilitates deoxygenation events, such as decarboxylation and dehydration, that eliminate oxygen from the biomass as CO, CO_2, and H_2O (Gogoi, Kumar and Lakshmi, 2023). Hence, plasma pyrolysis not only enhances the carbon content but also produces a char that is more hydrophobic and stable, making it highly desirable for a range of industrial applications.

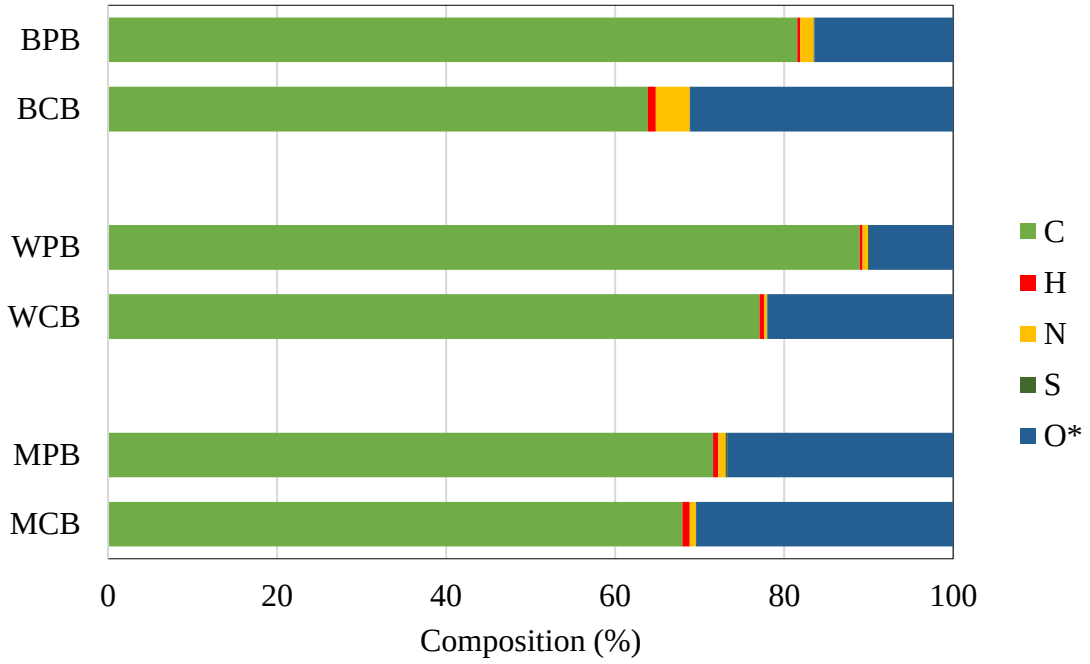

Figure 10. Elemental composition of biochar from different biomass

The results collectively emphasize the potential of plasma pyrolysis as a technique to produce biochar that is rich in carbon and has altered component compositions. The observed differences in elemental profiles among various biomass feedstocks emphasize the significance of taking into account biomass-specific properties while optimizing plasma pyrolysis conditions corresponding to these properties.

4. Conclusions

In summary, these findings highlight that the proximate composition of biochar is significantly affected by plasma pyrolysis, resulting in more hygroscopic and stable biochar with low moisture content and volatile matter while having high ash and fixed carbon content. The TGA analysis further supports this with high ash residue and late on-set temperature, thereby developing a better thermally stable carbon matrix. Some underlying mechanisms, including cross-linking, polymerization, and the formation of char layers promoted by the high-energy plasma environment could be attributed to the change in the thermal behavior of plasma pyrolyzed biochar. The heat flow characteristics from the DSC curve show that plasma pyrolyzed biochar possesses a unique thermal transition with a less pronounced broader endothermic peak, particularly occurring after its on-set temperature. However, the result was not consistent across biomass types, possibly due to the different makeup of chemicals inherent to each biomass. Plasma pyrolysis produces biochar with a significantly low specific surface area yet boasts a notably larger pore size over conventional pyrolysis regardless of biomass type. T-plot analysis showed that plasma pyrolyzed biochar had the lowest micropore volume, aligning with the observed lower specific surface area. This change can be ascribed to structural collapse due to raid heating, special gas phase reactions due to swift devolatilization, and surface chemistry alterations associated with the presence of several reactive species. SEM images showed a distinct morphological change for all plasma pyrolyzed char compared to the conventional counterpart. Although there was a slight difference among biomass types, plasma pyrolyzed biochar generally has a smoother overall texture and fewer irregularities dominated by meso- and macropores. Plasma pyrolysis significantly enhances carbon content across all biomass types, with the most pronounced effect observed in wood and BSG. The result indicates the ability of plasma pyrolysis to break down organic matter efficiently into carbon-rich solids (i.e., biochar). The high-energy plasma environment enhances aromaticity and facilitates deoxygenation events, resulting in a significant reduction of oxygen, thereby yielding a more hydrophobic and stable char. The findings collectively demonstrate that high-frequency plasma pyrolysis significantly affects the physicochemical properties of biochar, with slight differences across biomass types. Hence, it can be a promising alternative for tailoring biochar properties to meet specific applications.

Bibliography

About biochar | nordic biochar network (no date). Available at: https://www.nordicbiochar.org/biochar/ (Accessed: 5 August 2024).

Adeniyi, A.G., Ighalo, J.O. and Onifade, D.V. (2021) 'Production of Bio-Char from Plantain (musa Paradisiaca) Fibers Using an Updraft Biomass Gasifier with Retort Heating', *Combustion Science and Technology*, 193(1), pp. 60–74. Available at: https://doi.org/10.1080/00102202.2019.1650269.

Agun, L. *et al.* (2022) 'Plasma Technology in Waste-to-Energy Valorization: Fundamentals, Current Status, and Future Directions', *Handbook of Waste Biorefinery: Circular Economy of Renewable Energy*, pp. 813–830. Available at: https://doi.org/10.1007/978-3-031-06562-0_30/FIGURES/5.

Alkharabsheh, H.M. *et al.* (2021) 'Biochar and Its Broad Impacts in Soil Quality and Fertility, Nutrient Leaching and Crop Productivity: A Review', *Agronomy 2021, Vol. 11, Page 993*, 11(5), p. 993. Available at: https://doi.org/10.3390/AGRONOMY11050993.

Altıkat, Alperay *et al.* (2024) 'A Comprehensive Study of Biochar Yield and Quality Concerning Pyrolysis Conditions: A Multifaceted Approach', *Sustainability 2024, Vol. 16, Page 937*, 16(2), p. 937. Available at: https://doi.org/10.3390/SU16020937.

Alvarado-Flores, J.J. *et al.* (2024) 'Thermochemical Production of Hydrogen from Biomass: Pyrolysis and Gasification', *Energies 2024, Vol. 17, Page 537*, 17(2), p. 537. Available at: https://doi.org/10.3390/EN17020537.

Ambroz, Filip *et al.* (2018) 'Evaluation of the BET Theory for the Characterization of Meso and Microporous MOFs', *Small Methods*, 2(11), p. 1800173. Available at: https://doi.org/10.1002/SMTD.201800173.

Aminu, I., Nahil, M.A. and Williams, P.T. (2022) 'Hydrogen Production by Pyrolysis-Nonthermal Plasma/Catalytic Reforming of Waste Plastic over Different Catalyst Support Materials', *Energy and Fuels*, 36(7), pp. 3788–3801. Available at: https://doi.org/10.1021/ACS.ENERGYFUELS.1C04186/ASSET/IMAGES/LARGE/EF1C04186_0014.JPEG.

Analysis of Surface Area and Porosity in Biochar - Celignis Biomass Laboratory (no date). Available at: https://www.celignis.com/biochar-surface-area.php (Accessed: 5 August 2024).

Antonangelo, J.A. *et al.* (2019) 'Physicochemical properties and morphology of biochars as affected by feedstock sources and pyrolysis temperatures', *Biochar*, 1(3), pp. 325–336. Available at: https://doi.org/10.1007/S42773-019-00028-Z/METRICS.

Armah, E.K. *et al.* (2022) 'Biochar: Production, Application and the Future', *Biochar - Productive Technologies, Properties and Applications* [Preprint]. Available at: https://doi.org/10.5772/INTECHOPEN.105070.

Al Arni, S. (2018) 'Comparison of slow and fast pyrolysis for converting biomass into fuel', *Renewable Energy*, 124, pp. 197–201. Available at: https://doi.org/10.1016/J.RENENE.2017.04.060.

Azwar, E. *et al.* (2022) 'Progress in thermochemical conversion of aquatic weeds in shellfish aquaculture for biofuel generation: Technical and economic perspectives', *Bioresource Technology*, 344, p. 126202. Available at: https://doi.org/10.1016/J.BIORTECH.2021.126202.

Bao, X. *et al.* (2021) 'Hygroscopic Water Retention and Physio-Chemical Properties of Three In-House Produced Biochars from Different Feedstock Types: Implications on Substrate Amendment in Green Infrastructure', *Water 2021, Vol. 13, Page 2613*, 13(19), p. 2613. Available at: https://doi.org/10.3390/W13192613.

Batista, E.M.C.C. *et al.* (2018) 'Effect of surface and porosity of biochar on water holding capacity aiming indirectly at preservation of the Amazon biome', *Scientific Reports 2018 8:1*, 8(1), pp. 1–9. Available at: https://doi.org/10.1038/s41598-018-28794-z.

Bhatt, K.P. *et al.* (2022) 'A critical review on solid waste treatment using plasma pyrolysis technology', *Chemical Engineering and Processing - Process Intensification*, 177, p. 108989. Available at: https://doi.org/10.1016/J.CEP.2022.108989.

Biochar: Properties and Potential (no date). Available at: https://extension.psu.edu/biochar-properties-and-potential (Accessed: 5 August 2024).

Cha, J.S. *et al.* (2016) 'Production and utilization of biochar: A review', *Journal of Industrial and Engineering Chemistry*, 40, pp. 1–15. Available at: https://doi.org/10.1016/J.JIEC.2016.06.002.

Chakraborty, Jyoti Prasad *et al.* (2021) 'Biomass Pyrolysis: Current Status and Future Prospects', pp. 37–60. Available at: https://doi.org/10.1007/978-981-16-1888-8_3.

Chen, D. *et al.* (2016) 'Effect of pyrolysis temperature on the chemical oxidation stability of bamboo biochar', *Bioresource Technology*, 218, pp. 1303–1306. Available at: https://doi.org/10.1016/J.BIORTECH.2016.07.112.

Chen, G. *et al.* (2022) 'Plasma pyrolysis for a sustainable hydrogen economy', *Nature Reviews Materials 2022 7:5*, 7(5), pp. 333–334. Available at: https://doi.org/10.1038/s41578-022-00439-8.

Chen, H. *et al.* (2021) 'Review of low-temperature plasma nitrogen fixation technology', *Waste Disposal and Sustainable Energy*, 3(3), pp. 201–217. Available at: https://doi.org/10.1007/S42768-021-00074-Z/METRICS.

Chen, W. *et al.* (2019) 'Past, present, and future of biochar', *Biochar 2019 1:1*, 1(1), pp. 75–87. Available at: https://doi.org/10.1007/S42773-019-00008-3.

Cheng, Yan *et al.* (2015) 'Experimental Study on Coal Tar Pyrolysis in Thermal Plasma', *Plasma Chemistry and Plasma Processing*, 35(2), pp. 401–413. Available at: https://doi.org/10.1007/S11090-014-9608-3/FIGURES/7.

Costa, L.J. *et al.* (2024) 'Physical–chemical properties and hygroscopicity of Brazilian metallurgical charcoal', *Wood Science and Technology*, 58(2), pp. 503–532. Available at: https://doi.org/10.1007/S00226-024-01529-2/FIGURES/14.

Daghagheleh, O. *et al.* (2023) 'Feasibility of a Plasma Furnace for Methane Pyrolysis: Hydrogen and Carbon Production', *Energies 2024, Vol. 17, Page 167*, 17(1), p. 167. Available at: https://doi.org/10.3390/EN17010167.

Danesh, P. *et al.* (2023) 'Biochar Production: Recent Developments, Applications, and challenges', *Fuel*, 337, p. 126889. Available at: https://doi.org/10.1016/J.FUEL.2022.126889.

Devi, M. and Rawat, S. (2020) ‘A comprehensive review of the pyrolysis process: from carbon nanomaterial synthesis to waste treatment’, *Oxford Open Materials Science*, 1(1). Available at: https://doi.org/10.1093/OXFMAT/ITAB014.

EBC (2012-2023) (2022) *European Biochar Certificate - Guidelines for a Sustainable Production of Biochar*. Frick, Switzerland.

Elkhalifa, S. *et al.* (2022) ‘Pyrolysis of Biosolids to Produce Biochars: A Review’, *Sustainability 2022, Vol. 14, Page 9626*, 14(15), p. 9626. Available at: https://doi.org/10.3390/SU14159626.

Fang, H. *et al.* (2020) ‘Surface Micro-morphology and Adsorption Properties of Sediment Particles’, *Mechanics of Bio-Sediment Transport*, pp. 1–79. Available at: https://doi.org/10.1007/978-3-662-61158-6_1.

Ferraro, G. *et al.* (2024) ‘Biochar from lab-scale pyrolysis: influence of feedstock and operational temperature’, *Biomass Conversion and Biorefinery*, 14(5), pp. 5901–5911. Available at: https://doi.org/10.1007/S13399-021-01303-5/TABLES/2.

Gabhane, J.W. *et al.* (2020) ‘Recent trends in biochar production methods and its application as a soil health conditioner: a review’, *SN Applied Sciences 2020 2:7*, 2(7), pp. 1–21. Available at: https://doi.org/10.1007/S42452-020-3121-5.

Galarneau, A. *et al.* (2003) ‘Microporosity and connections between pores in SBA-15 mesostructured silicas as a function of the temperature of synthesis’, *New Journal of Chemistry*, 27(1), pp. 73–79. Available at: https://doi.org/10.1039/B207378C.

GANESH PRASAD, K.S., NEMA, S.K. and JAIN, V. (2007) ‘Plasma pyrolysis system and process for the disposal of waste using graphite plasma torch’.

Goebel, D.M. and Katz, I. (2008) ‘Basic Plasma Physics’, *Fundamentals of Electric Propulsion*, pp. 37–90. Available at: https://doi.org/10.1002/9780470436448.CH3.

Gogoi, D., Kumar, M. and Lakshmi, Y.G. (2023) ‘A Comprehensive Review on “Pyrolysis” for Energy Recovery’, *BioEnergy Research 2023 16:3*, 16(3), pp. 1417–1437. Available at: https://doi.org/10.1007/S12155-023-10568-9.

Hansen, V. *et al.* (2015) ‘Gasification biochar as a valuable by-product for carbon sequestration and soil amendment’, *Biomass and Bioenergy*, 72, pp. 300–308. Available at: https://doi.org/10.1016/J.BIOMBIOE.2014.10.013.

Harrish, A.M.J.C. and Pawar, H.S. (2022) ‘Role of Biochar in the Removal of Organic and Inorganic Contaminants from Wastewater’, *Biochar and its Application in Bioremediation*, pp. 107–134. Available at: https://doi.org/10.1007/978-981-16-4059-9_6/TABLES/3.

Hussain, M. *et al.* (2023) ‘Recent advances in dynamic modeling and control studies of biomass gasification for production of hydrogen rich syngas’, *RSC Advances*, 13(34), pp. 23796–23811. Available at: https://doi.org/10.1039/D3RA01219K.

Ippolito, J.A. *et al.* (2020) ‘Feedstock choice, pyrolysis temperature and type influence biochar characteristics: a comprehensive meta-data analysis review’, *Biochar*, 2(4), pp. 421–438. Available at: https://doi.org/10.1007/S42773-020-00067-X/TABLES/6.

Jiang, H. *et al.* (2021) 'Effects of torrefaction conditions on the hygroscopicity of biochars', *Journal of the Energy Institute*, 96, pp. 260–268. Available at: https://doi.org/10.1016/J.JOEI.2021.03.018.

John, N. *et al.* (2023) 'Physical Conversion of Biomass: Dewatering, Drying, Size Reduction, Densification, and Separation', *Handbook of Biomass*, pp. 1–28. Available at: https://doi.org/10.1007/978-981-19-6772-6_37-1.

Ke, L. *et al.* (2024) 'Microwave catalytic pyrolysis of biomass: a review focusing on absorbents and catalysts', *npj Materials Sustainability 2024 2:1*, 2(1), pp. 1–20. Available at: https://doi.org/10.1038/s44296-024-00027-7.

Khawkomol, S. *et al.* (2021) 'Potential of Biochar Derived from Agricultural Residues for Sustainable Management', *Sustainability 2021, Vol. 13, Page 8147*, 13(15), p. 8147. Available at: https://doi.org/10.3390/SU13158147.

Kwon, S. and Im, S. kyun (2022) 'Feasibility of non-thermal plasma gasification for a waste-to-energy power plant', *Energy Conversion and Management*, 251, p. 114978. Available at: https://doi.org/10.1016/J.ENCONMAN.2021.114978.

Leng, L. *et al.* (2021) 'An overview on engineering the surface area and porosity of biochar', *Science of The Total Environment*, 763, p. 144204. Available at: https://doi.org/10.1016/J.SCITOTENV.2020.144204.

Li, J. *et al.* (2016) 'Biochar from microwave pyrolysis of biomass: A review', *Biomass and Bioenergy*, 94, pp. 228–244. Available at: https://doi.org/10.1016/J.BIOMBIOE.2016.09.010.

Li, L. *et al.* (2023) 'Effects of pyrolysis temperature and feedstock type on biochar characteristics pertinent to soil carbon and soil health: A meta-analysis', *Soil Use and Management*, 39(1), pp. 43–52. Available at: https://doi.org/10.1111/SUM.12848.

Li, S. and Tasnady, D. (2023) 'Biochar for Soil Carbon Sequestration: Current Knowledge, Mechanisms, and Future Perspectives', *C 2023, Vol. 9, Page 67*, 9(3), p. 67. Available at: https://doi.org/10.3390/C9030067.

Li, T. *et al.* (2017) 'Experimental Comparison of Methane Pyrolysis in Thermal Plasma', *Plasma Chemistry and Plasma Processing*, 37(4), pp. 1033–1049. Available at: https://doi.org/10.1007/S11090-017-9806-X/FIGURES/10.

Lu, S. and Zong, Y. (2018) 'Pore structure and environmental serves of biochars derived from different feedstocks and pyrolysis conditions', *Environmental Science and Pollution Research*, 25(30), pp. 30401–30409. Available at: https://doi.org/10.1007/S11356-018-3018-7/FIGURES/6.

Maniraj, J. *et al.* (2023a) 'Introduction of Biochar: Sources, Composition, and Recent Updates', *Materials Horizons: From Nature to Nanomaterials*, Part F1442, pp. 1–17. Available at: https://doi.org/10.1007/978-981-99-5239-7_1/FIGURES/5.

Maniraj, J. *et al.* (2023b) 'Introduction of Biochar: Sources, Composition, and Recent Updates', *Materials Horizons: From Nature to Nanomaterials*, Part F1442, pp. 1–17. Available at: https://doi.org/10.1007/978-981-99-5239-7_1/FIGURES/5.

Miškovičová, Z. *et al.* (2024) 'An Overview Analysis of Current Research Status in Iron Oxides Reduction by Hydrogen', *Metals 2024, Vol. 14, Page 589*, 14(5), p. 589. Available at: https://doi.org/10.3390/MET14050589.

Murtaza, G. *et al.* (2024) 'Liming potential and characteristics of biochar produced from woody and non-woody biomass at different pyrolysis temperatures', *Scientific Reports 2024 14:1*, 14(1), pp. 1–12. Available at: https://doi.org/10.1038/s41598-024-61974-8.

Nair, R.R. *et al.* (2023) 'Biochar synthesis from mineral and ash-rich waste biomass, part 2: characterization of biochar and co-pyrolysis mechanism for carbon sequestration', *Sustainable Environment Research*, 33(1), pp. 1–17. Available at: https://doi.org/10.1186/S42834-023-00176-9/FIGURES/6.

Nepal, J. *et al.* (2023) 'Advances and prospects of biochar in improving soil fertility, biochemical quality, and environmental applications', *Frontiers in Environmental Science*, 11, p. 1114752. Available at: https://doi.org/10.3389/FENVS.2023.1114752/BIBTEX.

Nguyen, H.N. and Khuong, D.A. (2022) 'New Trends in Pyrolysis Methods: Opportunities, Limitations, and Advantages', *Engineered Biochar: Fundamentals, Preparation, Characterization and Applications*, pp. 105–126. Available at: https://doi.org/10.1007/978-981-19-2488-0_7/FIGURES/4.

Oliveira, F.R. *et al.* (2017) 'Environmental application of biochar: Current status and perspectives', *Bioresource Technology*, 246, pp. 110–122. Available at: https://doi.org/10.1016/J.BIORTECH.2017.08.122.

Ollegott, K. *et al.* (2020) 'Fundamental Properties and Applications of Dielectric Barrier Discharges in Plasma-Catalytic Processes at Atmospheric Pressure', *Chemie Ingenieur Technik*, 92(10), pp. 1542–1558. Available at: https://doi.org/10.1002/CITE.202000075.

Osman, A.I. *et al.* (2023) 'Reducing the carbon footprint of buildings using biochar-based bricks and insulating materials: a review', *Environmental Chemistry Letters 2023 22:1*, 22(1), pp. 71–104. Available at: https://doi.org/10.1007/S10311-023-01662-7.

Pahnila, M. *et al.* (2023) 'A Review of Pyrolysis Technologies and the Effect of Process Parameters on Biocarbon Properties', *Energies 2023, Vol. 16, Page 6936*, 16(19), p. 6936. Available at: https://doi.org/10.3390/EN16196936.

Palma, V. *et al.* (2020) 'A Review about the Recent Advances in Selected NonThermal Plasma Assisted Solid–Gas Phase Chemical Processes', *Nanomaterials*, 10(8), pp. 1–56. Available at: https://doi.org/10.3390/NANO10081596.

Panwar, N.L., Pawar, A. and Salvi, B.L. (2019) 'Comprehensive review on production and utilization of biochar', *SN Applied Sciences*, 1(2), pp. 1–19. Available at: https://doi.org/10.1007/S42452-019-0172-6/FIGURES/9.

Patra, B.R. *et al.* (2021) 'Biochar production, activation and adsorptive applications: a review', *Environmental Chemistry Letters 2021 19:3*, 19(3), pp. 2237–2259. Available at: https://doi.org/10.1007/S10311-020-01165-9.

Peng, Y. *et al.* (2021) 'Oxygen-Containing Functional Groups Regulating the Carbon/Electrolyte Interfacial Properties Toward Enhanced K+ Storage', *Nano-Micro Letters*, 13(1), pp. 1–15. Available at: https://doi.org/10.1007/S40820-021-00722-3/FIGURES/5.

Petersen, H.I. *et al.* (2023) 'Carbon stability and morphotype composition of biochars from feedstocks in the Mekong Delta, Vietnam', *International Journal of Coal Geology*, 271, p. 104233. Available at: https://doi.org/10.1016/J.COAL.2023.104233.

Plasma Activation of Biochar | Plasma Sources and Processing Lab (no date). Available at: https://www.egr.msu.edu/psp/projects/plasma-activation-biochar (Accessed: 8 August 2024).

Plasma classification (types of plasma) | Plasma-Universe.com (no date). Available at: https://www.plasma-universe.com/plasma-classification-types-of-plasma/ (Accessed: 6 August 2024).

Plasma Cutting Basics | Longevity (no date). Available at: https://www.longevity-inc.com/resources/resources/improving-your-skills/plasma-cutting-basics (Accessed: 6 August 2024).

Puri, L., Hu, Y. and Naterer, G. (2024) 'Critical review of the role of ash content and composition in biomass pyrolysis', *Frontiers in Fuels*, 2, p. 1378361. Available at: https://doi.org/10.3389/FFUEL.2024.1378361.

Qiu, M. *et al.* (2022) 'Biochar for the removal of contaminants from soil and water: a review', *Biochar*, 4(1), pp. 1–25. Available at: https://doi.org/10.1007/S42773-022-00146-1/FIGURES/7.

Rafiq, M.K. *et al.* (2016) 'Influence of Pyrolysis Temperature on Physico-Chemical Properties of Corn Stover (Zea mays L.) Biochar and Feasibility for Carbon Capture and Energy Balance', *PLOS ONE*, 11(6), p. e0156894. Available at: https://doi.org/10.1371/JOURNAL.PONE.0156894.

Rahman, M.M. *et al.* (2019) 'A Statistical Approach to Determine Optimal Models for IUPAC-Classified Adsorption Isotherms', *Energies 2019, Vol. 12, Page 4565*, 12(23), p. 4565. Available at: https://doi.org/10.3390/EN12234565.

Rajput, V. *et al.* (2024) 'Biochar production methods and their transformative potential for environmental remediation', *Discover Applied Sciences*, 6(8), pp. 1–15. Available at: https://doi.org/10.1007/S42452-024-06125-4/TABLES/2.

Ravindiran, G. *et al.* (2024) 'Production and modifications of biochar to engineered materials and its application for environmental sustainability: a review', *Biochar 2024 6:1*, 6(1), pp. 1–27. Available at: https://doi.org/10.1007/S42773-024-00350-1.

Regina, A. *et al.* (2024) 'Chemical Properties of Biomass', *Handbook of Biomass*, pp. 331–347. Available at: https://doi.org/10.1007/978-981-99-6727-8_12.

Ren, Z. *et al.* (2023) 'Effects of pore size, water content, and oxygen-containing functional groups on oxygen adsorption in bituminous coal', *Scientific Reports 2023 13:1*, 13(1), pp. 1–9. Available at: https://doi.org/10.1038/s41598-023-37632-w.

Rosenboom, J.G., Langer, R. and Traverso, G. (2022) 'Bioplastics for a circular economy', *Nature Reviews Materials 2022 7:2*, 7(2), pp. 117–137. Available at: https://doi.org/10.1038/s41578-021-00407-8.

Saeed, M.A. *et al.* (2016) 'Global kinetics of the rate of volatile release from biomasses in comparison to coal', *Fuel*, 181, pp. 347–357. Available at: https://doi.org/10.1016/J.FUEL.2016.04.123.

Sahoo, S.S. *et al.* (2021) 'Production and characterization of biochar produced from slow pyrolysis of pigeon pea stalk and bamboo', *Cleaner Engineering and Technology*, 3, p. 100101. Available at: https://doi.org/10.1016/J.CLET.2021.100101.

Scherdel, C., Reichenauer, G. and Wiener, M. (2010) 'Relationship between pore volumes and surface areas derived from the evaluation of N2-sorption data by DR-, BET- and t-plot',

Microporous and Mesoporous Materials, 132(3), pp. 572–575. Available at: https://doi.org/10.1016/J.MICROMESO.2010.03.034.

SEM Scanning Electron Microscopy - Scimed (no date). Available at: https://www.scimed.co.uk/education/sem-scanning-electron-microscopy/ (Accessed: 5 August 2024).

Siddiqui, M.Z. *et al.* (2022) 'Recent approaches on the optimization of biomass gasification process parameters for product H2 and syngas ratio: a review', *Environment, Development and Sustainability 2022*, pp. 1–29. Available at: https://doi.org/10.1007/S10668-022-02279-6.

SNEAD, L.L. (1999) 'Fusion Energy Applications', *Carbon Materials for Advanced Technologies*, pp. 389–427. Available at: https://doi.org/10.1016/B978-008042683-9/50014-5.

Suman, S. *et al.* (2018) 'Biochar Derived from Agricultural Waste Biomass Act as a Clean and Alternative Energy Source of Fossil Fuel Inputs', *Energy Systems and Environment* [Preprint]. Available at: https://doi.org/10.5772/INTECHOPEN.73833.

Świechowski, K. *et al.* (2022) 'Characterization of Engineered Biochar: Proximate Analyses, Ultimate Analyses, Physicochemical Analyses, Surface Analyses, and Molecular Analyses', *Engineered Biochar: Fundamentals, Preparation, Characterization and Applications*, pp. 127–148. Available at: https://doi.org/10.1007/978-981-19-2488-0_8/FIGURES/2.

The Use Of Argon In Plasma Cleaning (2023). Available at: https://www.sciplasma.com/post/argon-in-plasma-cleaning (Accessed: 6 August 2024).

Tomczyk, A., Sokołowska, Z. and Boguta, P. (2020) 'Biochar physicochemical properties: pyrolysis temperature and feedstock kind effects', *Reviews in Environmental Science and Biotechnology*, 19(1), pp. 191–215. Available at: https://doi.org/10.1007/S11157-020-09523-3/TABLES/3.

Uroić Štefanko, A. and Leszczynska, D. (2020) 'Impact of Biomass Source and Pyrolysis Parameters on Physicochemical Properties of Biochar Manufactured for Innovative Applications', *Frontiers in Energy Research*, 8, p. 532121. Available at: https://doi.org/10.3389/FENRG.2020.00138/BIBTEX.

Vanisree, G.S., Chandran, A.M. and Aparna, K. (2024) 'Investigation on thermochemical characteristics and pyrolysis kinetics of lignocellulosic biomass for biofuel production feasibility', *Biomass Conversion and Biorefinery*, pp. 1–19. Available at: https://doi.org/10.1007/S13399-024-05657-4/TABLES/3.

Vilas-Boas, A.C.M. *et al.* (2024) 'Valorisation of residual biomass by pyrolysis: influence of process conditions on products', *Sustainable Energy & Fuels*, 8(2), pp. 379–396. Available at: https://doi.org/10.1039/D3SE01216F.

Wang, J. and Wang, S. (2019) 'Preparation, modification and environmental application of biochar: A review', *Journal of Cleaner Production*, 227, pp. 1002–1022. Available at: https://doi.org/10.1016/J.JCLEPRO.2019.04.282.

Weber, K. and Quicker, P. (2018) 'Properties of biochar', *Fuel*, 217, pp. 240–261. Available at: https://doi.org/10.1016/J.FUEL.2017.12.054.

Wheeler, R.R., Jr. *et al.* (2012) 'Advanced Plasma Pyrolysis Assembly (PPA) Reactor and Process Development'.

Wnukowski, M. (2023) ‘Methane Pyrolysis with the Use of Plasma: Review of Plasma Reactors and Process Products’, *Energies 2023, Vol. 16, Page 6441*, 16(18), p. 6441. Available at: https://doi.org/10.3390/EN16186441.

Wu, P. *et al.* (2023) ‘Bibliometric analysis of biochar research in 2021: a critical review for development, hotspots and trend directions’, *Biochar 2023 5:1*, 5(1), pp. 1–21. Available at: https://doi.org/10.1007/S42773-023-00204-2.

Wu, Q. *et al.* (2017) ‘Characterization of products from hydrothermal carbonization of pine’, *Bioresource Technology*, 244, pp. 78–83. Available at: https://doi.org/10.1016/J.BIORTECH.2017.07.138.

Xiang, W. *et al.* (2022) ‘Microwave-assisted pyrolysis derived biochar for volatile organic compounds treatment: Characteristics and adsorption performance’, *Bioresource Technology*, 355, p. 127274. Available at: https://doi.org/10.1016/J.BIORTECH.2022.127274.

Xu, M. *et al.* (2023) ‘Biochar Decreases Fertilizer Leaching and Promotes Miscanthus Growth in Saline-Alkaline Soil’, *Plants*, 12(20), p. 3649. Available at: https://doi.org/10.3390/PLANTS12203649/S1.

Yaashikaa, P.R. *et al.* (2020) ‘A critical review on the biochar production techniques, characterization, stability and applications for circular bioeconomy’, *Biotechnology Reports*, 28, p. e00570. Available at: https://doi.org/10.1016/J.BTRE.2020.E00570.

Yadav, S. and Singh, D. (2023) ‘Assessment of biochar developed via torrefaction of food waste as feedstock for steam gasification to produce hydrogen rich gas’, *Carbon Research*, 2(1), pp. 1–13. Available at: https://doi.org/10.1007/S44246-023-00065-1/FIGURES/8.

Yang, H. *et al.* (2024) ‘Effect mechanism of phosphorous-containing additives on carbon structure evolution and biochar stability enhancement’, *Biochar*, 6(1), pp. 1–16. Available at: https://doi.org/10.1007/S42773-024-00330-5/FIGURES/8.

You, K. *et al.* (2021) ‘One-Step Preparation of Biochar Electrodes and Their Applications in Sediment Microbial Electrochemical Systems’, *Catalysts 2021, Vol. 11, Page 508*, 11(4), p. 508. Available at: https://doi.org/10.3390/CATAL11040508.

Zakaria, H.A. *et al.* (2017) ‘DEVELOPMENT OF WATER TREATMENT SACHETS FROM THE SEEDS OF MORINGA OLEIFERA AND ACTIVATED CARBON’, *MATTER: International Journal of Science and Technology*, 3(3), pp. 240–252. Available at: https://doi.org/10.20319/MIJST.2018.33.240252.

Zhai, Z. *et al.* (2023) ‘Pyrolytic gas analysis and evaluation from thermal plasma pyrolysis of simulated oil-based drill cuttings’, *Waste Disposal and Sustainable Energy*, 5(3), pp. 367–382. Available at: https://doi.org/10.1007/S42768-023-00153-3/FIGURES/11.

Zhang, X. *et al.* (2022) ‘Effect of pyrolysis temperature on composition, carbon fraction and abiotic stability of straw biochars: correlation and quantitative analysis’, *Carbon Research*, 1(1), pp. 1–14. Available at: https://doi.org/10.1007/S44246-022-00017-1/FIGURES/5.

Zhang, Y. *et al.* (2019) ‘Evolution of Char Structure During In-Situ Biomass Tar Reforming: Importance of the Coupling Effect Among the Physical-Chemical Structure of Char-Based Catalysts’, *Catalysts 2019, Vol. 9, Page 711*, 9(9), p. 711. Available at: https://doi.org/10.3390/CATAL9090711.

Zhang, Y. *et al.* (2022) ‘A review of biochar prepared by microwave-assisted pyrolysis of organic wastes’, *Sustainable Energy Technologies and Assessments*, 50, p. 101873. Available at: https://doi.org/10.1016/J.SETA.2021.101873.

Zoghlami, A. and Paës, G. (2019) ‘Lignocellulosic Biomass: Understanding Recalcitrance and Predicting Hydrolysis’, *Frontiers in Chemistry*, 7, p. 478626. Available at: https://doi.org/10.3389/FCHEM.2019.00874/BIBTEX.

Appendix

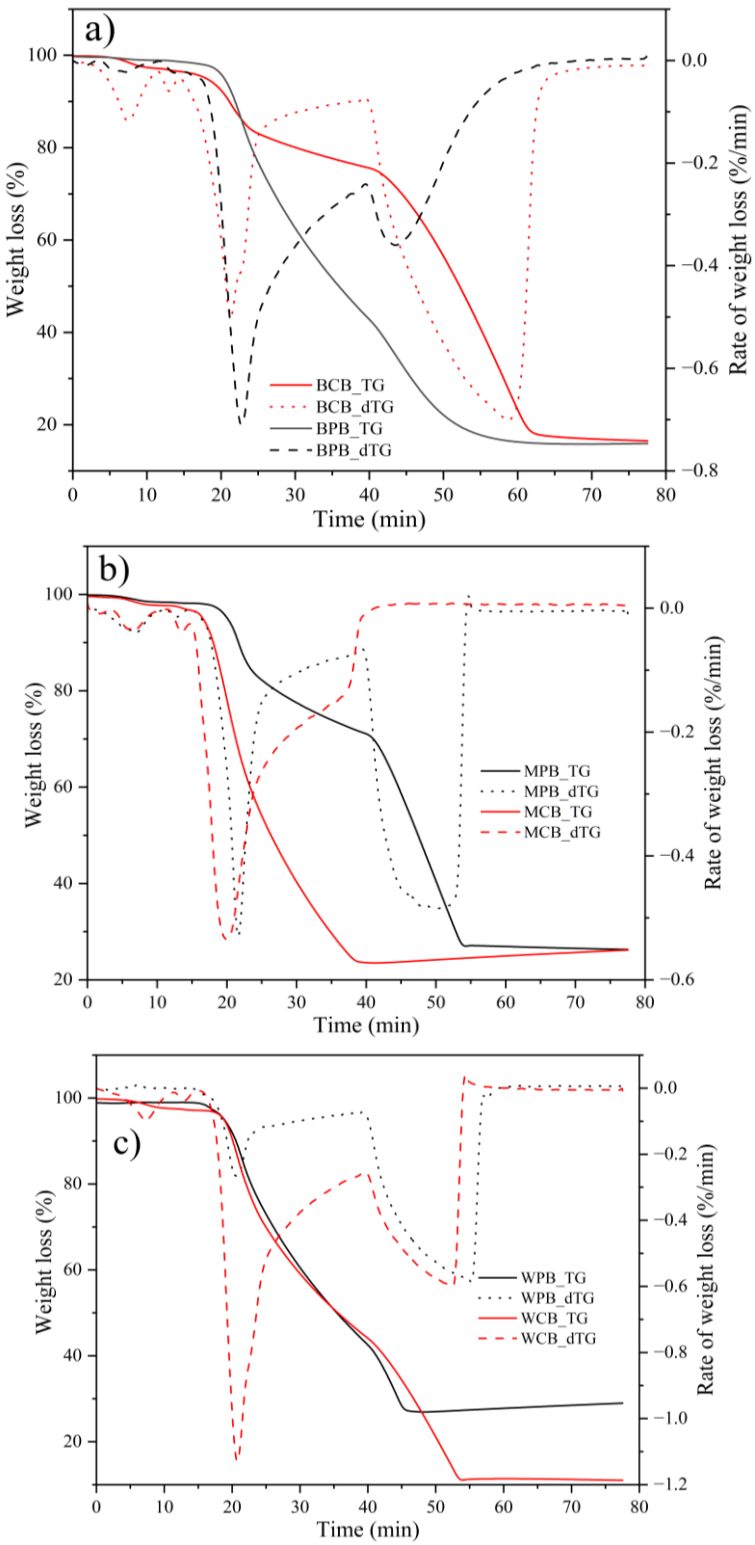

*Figure Appx.1. Thermogravimetric (TG) and derivative thermogravimetric (dTG) curves plotted against time for **a)** BSG-plasma pyrolyzed biochar (BPB) and BSG-conventionally pyrolyzed biochar (BCB), **b)** Miscanthus-plasma pyrolyzed biochar (MPB) and Miscanthus-conventionally pyrolyzed biochar (MCB) and **c)** and Smoke wood-plasma pyrolyzed biochar (WPB) and smoke wood-conventionally pyrolyzed biochar (WCB).*